BEHAVIOR AND STRENGTH OF MASONRY PRISMS LOADED IN COMPRESSION

by

Tamara Kaaki

Submitted in partial fulfilment of the requirements
for the degree of Master of Applied Science

at

Dalhousie University
Halifax, Nova Scotia
July 2013

To my parents

TABLE OF CONTENTS

LIST OF TABLES

LIST OF FIGURES

ABSTRACT

The compressive strength of masonry is the most important material property for the design of structural masonry. The behavior and strength of masonry prisms under compressive loading has been a fundamental research topic. In most practical applications, the compressive forces are applied normal to the masonry bed joint and thus the masonry compressive strength is obtained by subjecting the masonry prisms in compression normal to the bed joint in the experimentation. However, there are other masonry members that rely on the compressive strength of masonry either parallel or inclined with an angle to bed joints such as masonry beams or masonry infills. For the latter application, the current practice is to use a reduction factor χ in combination with compressive strength of masonry normal to the bed joint to account for the effect of loading direction on the compressive stress. Despite considerable research has been conducted on the masonry prism strength under compression normal to bed joints, the information on the effect of loading direction on the masonry prism strength is limited. Some conflicting findings have been reported by different researchers in terms of the value of the reduction factor.

An experimental program involving the test of 47 prisms and 27 square panels was therefore conducted to investigate the effects of a few influential parameters on the behavior and strength of masonry in compression. Parameters that were considered in the experimental program included loading orientation, height-to-thickness ratio, grouting arrangement, mortar strength, and central web interruption. Results from this study were used to augment the existing database and to verify the reduction factor for loading direction effect currently specified in the design standard. The unit-mortar method currently used in the standard for masonry compressive strength determination was also evaluated. Key observations are reported and recommendations are made as appropriate.

LIST OF ABBREVIATIONS AND SYMBOLS USED

The following is a list of notations and symbols used in this thesis. All symbols and notations used are also defined in the text when they first appear.

Symbols

A_e	Effective cross-sectional area of masonry
A_n	Net area of masonry used in diagonal tensile stress calculation
A_g	Gross cross-sectional area of masonry
b	Overall web width
e	Eccentricity
$E_{b,}$ E_c	Modulus of elasticity of beam, column
E_{bc}	Modulus of elasticity of bounding columns
$E_{f,}$ E_m	Young's elastic modulus of the frame, infill
$(EI)_{eff}$	Effective stiffness of wall
f'_m	Compressive strength of the masonry normal to the bed joint
f_{dt}	Diagonal tensile strength of masonry
h	Height of specimen
h_w	Height of infill wall
$I_{b,}$ I_c	Moment of inertia of the beam, column
I_{bc}	Moment of inertia of bounding columns
I_o	Moment of inertia of the effective cross-sectional area about its centroidal axis
l_w	Length of infill wall
l_d	Diagonal length of infill panel
k	Effective length factor for compressive member
n	Percent of the gross area that is solid
P	Compressive load applied
P_{cr}	Critical axial compressive load
P_d	Axial compressive load on the section under consideration
P_r	Factored axial load resistance
P_{CSA}	Ultimate load calculated using CSA equations
P_{EXP}	Ultimate load obtained from experiment results
P_{MSJC}	Ultimate load calculated using MSJC equations
r	General solution of a quadratic equation of eccentricity for the case where the edge of the stress block is within the tension flange of hollow masonry
t	Thickness of specimen
t_e	Effective thickness of infill wall
t_f	Thickness of the flange of unit
V_r	Factored shear resistance
w	Width of specimen
w_e	Effective width of diagonal strut calculated using CSA equations
w_{inf}	Width of diagonal strut calculated using MSJC equations
β_d	Ratio of factored dead load moment to total factored moment

θ	Angle of the diagonal strut measured from the horizontal
λ_{strut}	characteristic stiffness parameter
$\alpha_{L,}$ α_h	Horizontal, vertical contact length between the frame and the diagonal strut
ϕ_e	Resistance factor for member stiffness used in the determination of slenderness effects on the capacity of unreinforced masonry
ϕ_m	Resistance factor for masonry
χ	Factor used to account for direction of compressive stress in a masonry member relative to the direction used for the determination of $f'_{m.}$

Abbreviation

CMU	Concrete masonry unit
RC	Reinforced concrete
SCT	Structural clay tile
UB	British universal beams
UC	British universal columns

ACKNOWLEDGEMENT

I would like to express my deepest appreciation to all those who provided me the possibility to complete this dissertation.

Foremost, this dissertation would not have been possible without the guidance of my research advisor, Dr. Yi Liu who provided the vision, encouragement, and necessary advice for me to proceed through this program. There are no words that could express my sincerest appreciation for her patience and immense knowledge that have guided me through the entire process of this research.

My thanks also go to my thesis committee members Dr. George Jarjoura and Dr. Steve Zou for their time spent on reviewing this thesis. I would like to express my thanks to the faculty and staff of the Department of Civil and Resource Engineering for their help and assistance during the experimental portion of this research. A special thanks to Mr. Gerry Hubley for his hard work and assistance throughout the fabrication of the specimens.

Most importantly, my deepest gratitude goes to my beloved parents, Ghassan and Diana, my brother, Mahmoud, my grandparents and aunt for their endless love, prayers and support. Their love provided my inspiration and was my driving force. My sincerest appreciation and love goes to my guardian angel, Mona Sidawi Safadi, without whom I could not have made it here.

Special thanks to Mohammed Esmat who made me believe in myself and provided me with unconditional support and advice throughout this research. I will also never forget the confidence, strength and encouragement that my best friends, Samira Omar, Nada Tohme, Meredith Rudner and Siba Jaber, provided me throughout the years in order to achieve my goals. Also, I would like to also thank Abdulrahman ElKady and Xi Chen for their assistance.

CHAPTER 1 INTRODUCTION

1.1 BACKGROUND OF MASONRY

Masonry has been used to construct significant structures since the beginning of civilization (Drysdale and Hamid, 2005) for its durability and aesthetic reasons. In addition, fire and heat resistance and versatility make masonry, to this day, an appealing building material. However, the structural use of masonry experienced a decline in the past 100 years due to the slow development and implementation of rational design standards. While new construction techniques supported by design guidelines were developing for structural steel and reinforced concrete, the design of masonry was still largely based on the "rules of thumb" principles (Hatzinikolas and Korany, 2005). Not until 1950's, the introduction of the American Standards Association Building Code Requirements for Masonry (ASA A41.1-1953) and the National Building Code of Canada (1965) began the revival of masonry. At present, there are various codes and standards worldwide governing the design of masonry structures, most of which are based on limit state design philosophy. In Canada, the governing standard is CSA S304.1-04 (2004) for design of masonry structures whereas in US, the Masonry Structure Joint Committee (MSJC) adopted the TMS 402-11/ACI 530-11/ASCE 5-11 standard for masonry design, hereafter referred to as MSJC 2011.

1.2 COMPRESSIVE STRENGTH OF MASONRY

The behavior and strength of masonry prisms under compressive loading has been a fundamental research topic. The compressive strength of masonry is the most important mechanical property in design. Also, testing for the compressive strength of the component materials and of prisms is an essential quality control procedure used in construction. According to the CSA S304.1-04 and MSJC 2011, the compressive strength of masonry normal to the bed joint, f'_m, used in structural design is determined by two methods: Prism Test method and the Unit-Mortar Strength method. The first method is by experimentally subjecting the masonry prisms to direct compression to failure to determine the f'_m value. Masonry prisms are built as a representative of actual construction with a minimum height-to-thickness ratio requirement. Using the latter method, the f'_m value is obtained using tabulated values provided by the standards from knowledge of the

strength of the unit, mortar type and whether the units are hollow or fully grouted. The tabulated values provide a simple tool for the determination of the compressive strength; however this method is calibrated using test results obtained 40 years ago. Previous studies have shown that the tabulated values do not provide strength values consistent with the experimental results. An examination of the unit-mortar strength method is needed.

In addition to the compressive strength normal to the bed joint, the compressive strength of masonry either parallel or inclined with an angle to the bed joint is also of great interest as there are masonry members such as masonry beams or masonry infills that rely on the latter strength. Previous research has shown that masonry compressive strength parallel to the bed joint is considerably less than the compressive strength normal to the bed joint. The current Canadian design standard S304.1-04 recognizes this and specifies a factor of χ(= 0.5) to be used in combination with compressive strength of masonry normal to the bed joint to account for the effect of loading direction on the compressive stress. Despite considerable research has been conducted on the masonry prism strength under compression normal to bed joints, the information on the effect of loading direction on the masonry prism strength is limited. Some recent testing programs reported in the literature have shown conflicting results with the suggested χ factor. Therefore, this research is also aimed to investigate experimentally the behavior and strength of masonry prisms subjected to compression parallel to the bed joint.

1.3 RESEARCH OBJECTIVE

The objectives of this experimental study include the following:

1. To conduct an extensive literature review on the research in the topic of masonry prisms and masonry infilled walls.
2. To conduct an experimental study of masonry prisms under compressive loading in two directions.
3. To analyze the effect of several influential parameters on the compressive strength of masonry.
4. To assess the validity of the tabulated "Unit-Mortar Strength" method provided by the Canadian masonry design standard CSA S304.1-04 and American code MSJC 2011 with the results of this experimental study.

5. To analyze the relationship of loading direction and determining a factor χ using results of this experimental study.
6. To assess the validity of using the factor χ (=0.5) provided by Canadian code CSA S304.1-04 with reported experimental results on infill walls by other researchers.
7. To present appropriate conclusions and recommendations resulting from this research.

1.4 ORGANIZATION OF REPORT

A comprehensive literature review relevant to the subject of masonry prisms loaded in two directions was conducted and presented in Chapter 2 on the design of masonry prisms and masonry infilled walls. Chapter 3 presents a detailed description of the experimental program which included various auxiliary tests on masonry components, as well as the testing of 47 prisms and 27 panels. Chapter 4 discusses the results obtained from the experimental program of the auxiliary tests and prism and panel tests. Comparisons between the experimental and tabulated values in the codes were performed and discussed in Chapter 5. In addition, calculations and comparisons between analytical and experimental results obtained from literature on infill walls are found in Chapter 5. Chapter 6 presents the summary and conclusions of the research. Appendix A presents a detailed example for determining the strength of infill walls using the methods provided in the design codes.

CHAPTER 2 LITERATURE REVIEW

2.1 INTRODUCTION

The main objective of this study is to investigate the behavior and strength of masonry prisms with the focus on the effect of the loading direction. The findings are incorporated in evaluating the in-plane strength of masonry infills. The following literature review attempts to summarize the existing research on behavior and strength of masonry prisms and the in-plane strength of masonry infills.

2.2 BEHAVIOR OF MASONRY PRISMS

Masonry has been used primarily as the gravity load bearing material to resist compression. For example, masonry walls and columns are designed to resist vertical loads. Therefore, the compressive strength of masonry prisms is the most important property required in the design of structural masonry. In this case, the compressive forces are applied normal to the bed joint and thus the masonry compressive strength f'_m is obtained by subjecting the masonry prisms in compression normal to the bed joint in the experimentation. However, there are other masonry members, such as beams and flexural walls spanning horizontally which rely on the compressive strength of masonry parallel to bed joints.

Masonry prism behavior and strength under vertical loading has been a fundamental research topic for the past six decades and many influential parameters on the prism strength have been researched in the form of experimentation and numerical modeling. A detailed literature review is provided in Section 2.2.2. The following gives a basic understanding of the behavior of masonry prisms. Figure 2.1 shows a schematic diagram of a prism test specimen.

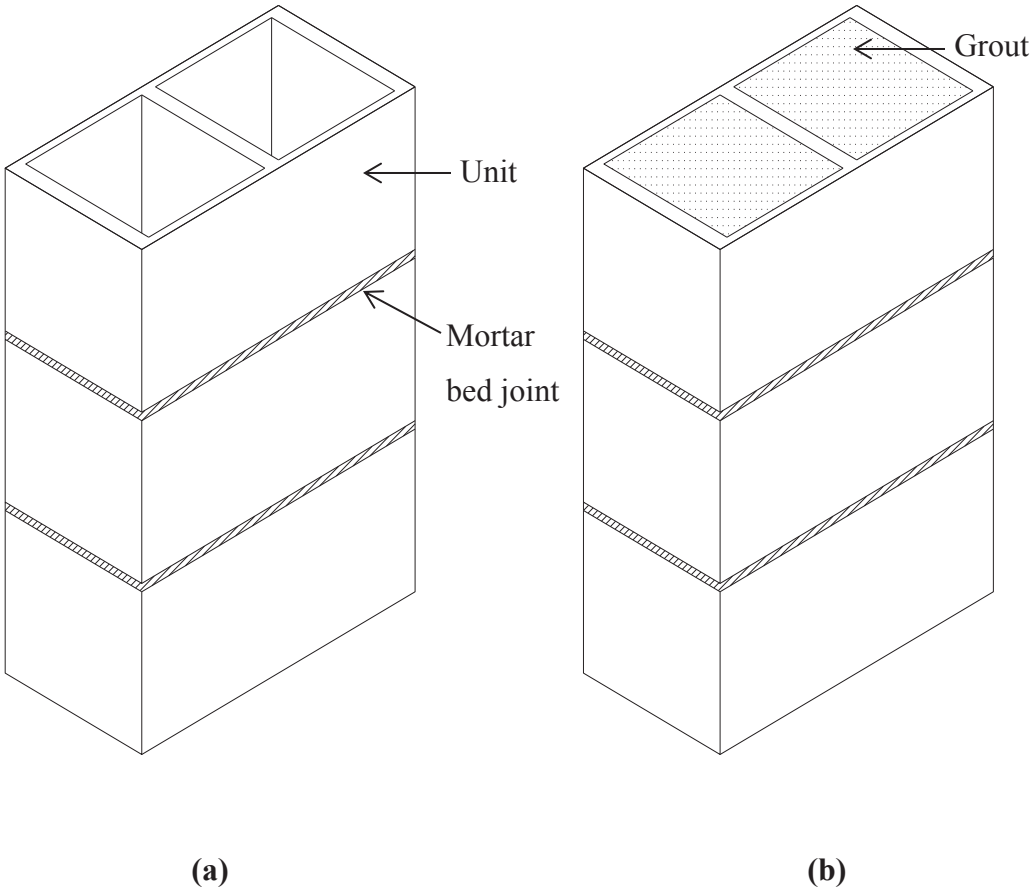

Figure 2.1 Schematic diagram of (a) hollow prism and (b) grouted prism

It has been established that the compressive strength of the masonry assemblage differs from the compressive strength of individual components of the prism. Typical compressive strength of masonry units is relatively high but the compressive strength of mortar is low. The resulted prism strength is found to be somewhere in between.

Two failure modes are commonly observed for masonry prisms in compression. One is masonry crushing for weak units and the other is the vertical cracking through either the face-shell or web of the prism. For the latter mode, the vertical compressive stresses applied are transferred to the mortar, which results in the mortar expanding laterally. The masonry unit resists the expansion of the mortar and thus creates lateral confined compressive stresses in the mortar and lateral tensile stresses in the unit. Due to the low tensile strength of the masonry, cracking through the flange or web of the units is formed which results in the final failure of the prism. In addition, when the

prisms are filled with grout, the incompatibility of the stress-strain properties of the grout with the block causes additional lateral strain on the block.

Previous research (Drysdale and Hamid 1980; Lee et al. 1984; Khalaf 1997) showed that the compressive strength of masonry parallel to the bed joint is less than the compressive strength of masonry normal to the bed joint. When the stresses are applied parallel to the bed joints, Drysdale and Hamid (1980) and Lee et al. (1984) found that ungrouted prisms exhibited vertical splitting across the central webs due to tensile stresses that is developed within the blocks. While Drysdale and Hamid (1980) reported that grouted prisms displayed a similar failure mode as ungrouted prisms, Lee et al. (1984) observed otherwise. Lee et al. (1984) noted that for ungrouted prisms failure was sudden and horizontal cracks were developed in the flanges of the units near the loaded surface, these cracks diminished towards the mid-height of the prism. For grouted prisms the mortar joint failed at an early stage and the prisms experienced severe cracking of the bed joints and cracking or crushing of the head joints. Figure 2.1 outlines the stress-strain relationship for both prisms with loading normal and parallel to the bed joint.

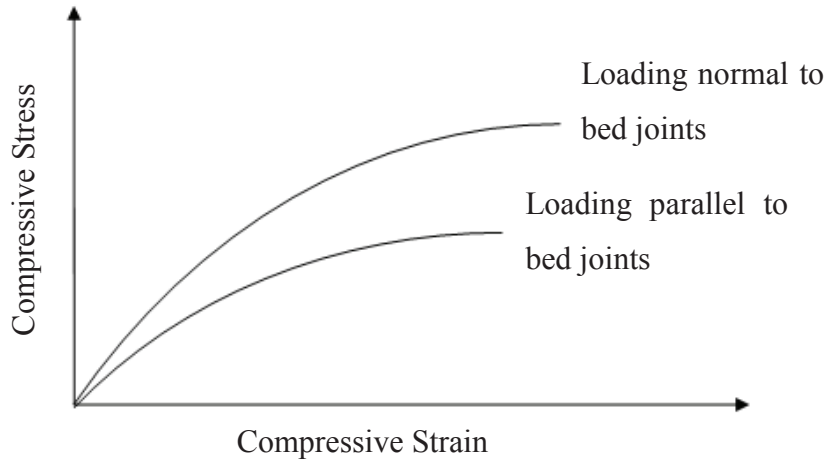

Figure 2.2 Schematic stress-strain relationships for masonry prisms subjected to loading parallel and normal to the bed joints

2.2.1 CSA S304.1-04 and MSJC 2011 Guidelines

In Canada, the design of masonry structures is governed by CSA S304.1-04 (2004) and the masonry material testing methods and specifications are covered in various CSA standards. In the United States, the Masonry Structures Joint Committee (MSJC) is responsible for design provisions of masonry structures and the material testing methods and specifications are specified in various ASTM standards. CSA S304.1 Annex D provides requirements and procedures for determining the compressive strength of masonry prisms. These test methods are similar in many respects to corresponding ASTM standards (ASTM C1314, C1072 2011). In addition, ASTM E519 (2010) describes the test requirements to determine the tensile strength of masonry when loaded in diagonal compression.

Strength of mortar and grout for engineered masonry shall be determined in accordance with the requirements of CSA A179 (2004). ASTM C270 and ASTM C476 provide similar requirements and proportioning procedures for both mortar and grout respectively.

The prism compressive strength is calculated by dividing the failure load at the 28-day age by the effective cross-sectional area, A_e, an area that includes the area of cores filled with grout. Both CSA S304.1-04 and ASTM C1314 specify a correction factor for specified f'_m to account for the height-to-thickness ratios, h/t, of prisms. The correction factors specified by CSA S304.1-04 are for different types of masonry units taking into account the presence of grout. These factors are considered to be conservative values for most prisms. The CSA S304.1-04 recommends the use of prisms with height-to-thickness ratio close to 5. For other values of ratio, correction factors which are less than unity are used. In ASTM C1314 (2011), the specified correction factors are different from CSA values and they are for a general masonry prism without stating type of masonry unit or the grouting condition.

The CSA S304.1-04 (2004) specifies a factor χ to be used in combination with f'_m to account for the effect of loading direction on the compressive stress. When the compressive forces are applied parallel to the bed joint and the grout is not horizontally continuous in the zone of compression, the factor χ is to be 0.5. When the compressive forces are applied parallel to the bed joint and the grout is horizontally continuous in the zone of compression, the factor χ is

considered to be 0.7. The factor χ is considered to be unity when the compressive forces are applied normal to bed joint.

2.2.2 Previous Research - Masonry Compressive Strength

Hegemier et al. (1978) investigated the compressive strength of concrete masonry prisms normal to the bed joint. The authors found that prism strength was primarily a function of the number of bed joints and not the h/t ratio. Bond pattern was observed to have an effect on strength. The authors recommended that prisms be constructed from four or five courses with either three or four mortar bed joints.

Drysdale and Hamid (1979) performed 146 axial compression tests on concrete block masonry prisms and established that a 3-course block prism is preferred to 2-course high block to represent the behavior close to a real wall. It was found that Type N mortar, which has lower strength than Type S mortar, only resulted in a 10% decrease in prism strength and a large increase in grout strength resulted in a relatively small increase in prism capacity.

Boult (1979) aimed to determine a relationship between the compressive strength and the height of concrete masonry prisms made of different types of masonry blocks. A series of stack bonded prisms with h/d (height-to-least lateral dimension) of 2 to 5 were constructed for each masonry unit type. Test results showed that the compressive strength decreased as the prism height increased and the rate of decline was dependent on the block type. Results also showed that the decrease in strength as height increased appeared to be insignificant between the 5- course high prisms and the 12- course high columns. Boult suggested that careful consideration of the material properties of the units and grout should be taken into account when assembling the prisms.

Drysdale and Hamid (1980) studied the failure modes and strength of both the concrete and brick masonry prisms when subjected to compression applied at designated angles in relation to the bed joint. Axial compression both parallel and normal to the bed joint was considered as well as θ of 15º, 45º and 75º. Regular flat ended concrete blocks, Type S mortar and a medium strength grout was used for all prisms. Results showed that grout had a maximum contribution for θ= 15º

and no significant contribution for θ= 75º. It was observed that two major failures were exhibited for both ungrouted and grouted prisms; a shear mode failure along the bed or head joint and a tensile failure of the prism. For θ=15º, large shear stresses and small normal stresses were developed along the bed joint resulting into a shear-slip failure. For θ= 75 º, high shear stresses and low normal stresses along the head joint resulted in a shear-tension failure. For θ= 45º, a mixed shear-tension mode of failures was developed since shear and normal stresses were balanced along the bed and head joints. The maximum prism strength was achieved when prisms were compressed at an angle normal to the bed joint. The authors underlined the importance of considering the effects of the stress orientation along the bed joint when determining the strength of masonry in design.

Brown and Whitlock (1982) showed that high strength grout and mortar, high tensile strength brick and low brick coring percentage are several factors that increased prism strength. For most prisms tested, it was found that the simple superposition of the strength of grouted core and the hollow brick prisms overestimates the strength and the contribution from the grout.

Lee et al. (1984) tested 82 grouted and ungrouted concrete masonry prisms under compression both parallel and perpendicular to the bed joints. The effects of several parameters on the compressive strength in the two different loading orientations considered were the mortar and grout strength, and head mortar joint detail. The authors noted that for prisms loaded parallel to the bed joint, the head joint had a significant effect on the behavior of the prism and was recommended that the head joints be completely filled. The mortar strength was found to be an important parameter in affecting the strength of prisms loaded parallel to the bed joint; a maximum increase in prism strength of 52% is noted with the use of a stronger mortar. A significant increase in grout strength is found to have a small effect on prism strength.

Wong and Drysdale (1985) tested prisms made from hollow, solid and grouted concrete block units subjected to compression both normal and parallel to the bed joint. Prisms of 2 to 5 courses high were tested for both hollow and grouted concrete block units. Two types of blocks were used to build the prisms, a 190 mm two-cell stretcher unit and a solid 190 mm block. Type S mortar and a medium strength grout were used in all prisms. The authors found that the compression parallel to the bed joint is 25% lower than the compression normal to the bed joint.

In addition, they confirmed that grouted and solid prisms exhibited 35% lower strength than hollow prisms and this is valid for both loading directions. Wong and Drysdale recommended that design standards should take into account the properties of the prisms for all directions of compression forces and treat the prisms separately.

Using experimental and numerical modeling Guo (1991) assessed various parameters and their influence on the mechanical properties of masonry units and assemblages under several loading conditions. Guo found that prism strength is higher for prisms subjected to compression normal to the bed joint than parallel to the bed joint. Furthermore, the cracking load was also lower for compression parallel to the bed joint. For compression normal to the bed joint, typical prisms were laid in running bond with face shell mortar bedding using hollow concrete block units and type S mortar. For compression parallel to the bed joint, the author does not state whether or not the cross-sectional area was based on full or face shell mortar bedding, but indicates that ultimate strength calculation was based on minimum cross-sectional area. Guo noted that for compression parallel to the bed joint, the bed joint thickness is not a controlling factor affecting prism strength but the head joint thickness is. It was found that unit strength has a larger effect on prism strength when compression is parallel to the bed joint than normal to the bed joint. Increasing block strength from normal to strong increases the prism strength by 22% and 35% for compression normal and parallel to the bed joint, respectively.

Khalaf (1997) investigated the strength and behavior of grouted and ungrouted prisms and blocks when subjected to compression both normal and parallel to the bed joint. The author found that increasing mortar strength increased prism strength in both direction of loading. However, the effect of increasing mortar strength on prism strength was not significant for prisms compressed parallel to the bed joint. It was observed an increase in grout strength leads to an increase in compressive strength for prisms compressed normal to the bed joint; whereas prisms compressed parallel to the bed joint exhibited a decrease in strength for high strength grout. Khalaf (1997) found that strength of grouted blockwork masonry compressed parallel to the bed joint was in the range of 16-42% less than that when compressed normal to the bed face.

Bennett et al. (1997) conducted tests on 23 structural clay tile prisms subjected to axial compression. The force was applied at an angle θ of 0º, 22.5 º, 45 º, 67.5 º and 90 º with the bed

joint. Mortar strength was observed to have little effect on prism strength. Prisms strength when loaded normal to the bed joint was estimated to be three-tenth the unit tile strength. Prisms loaded at $\theta = 0^{o}$, normal to the bed joint, showed maximum prism strength, while prisms loaded at $\theta = 67.5^{o}$ showed minimum strength.

Korany and Glanville (2005) compared the procedure for calculating the compressive strength of masonry in the American, Canadian, British and Australian codes. The authors concluded that the tabulated f'_m values varied between the codes and were not representative of measured values. Also, as unit strength increased, the variation between the codes increased.

Haach et al. (2010) investigated the compressive strength of concrete block masonry when subjected to uniaxial compression loads. When the specimens were loaded in compression parallel to the bed joints, cracking along the mortar-block interface was observed due to the tensile stresses that are developed normal to the bed joint. The authors noted that the compressive strength parallel to the bed joint is about 55% of the compressive strength normal to the bed joint.

Soon (2011) tested concrete masonry block prism subjected to loading either normal or parallel to the bed joint. Type S mortar was used and prisms where either grouted, partially grouted or fully grouted. When loaded parallel to the bed joint, hollow square prisms showed higher compressive strength than fully grouted square prisms. The compressive strength of the prisms when loaded normal to the bed joint was found to be approximately 50% higher than prisms loaded parallel to the bed joint.

2.2.3 Previous Research - Masonry Tensile Strength

In the context of in-plane strength of masonry infills, the infill is subjected to lateral loading and vertical loading as a result of the frame confinement. This combined loading produces principal tension stresses in the wall leading to tensile cracking when the tensile strength is exceeded. In addition to the development of horizontal and vertical cracks corresponding to tension normal or parallel to the bed joints, various forms of diagonal cracking can occur. This cracking is

dependent on the combination of principal stress, orientation of principal stress with respect to the mortar joints, and various material properties.

Three main test methods have been developed to determine the capacity of masonry assemblages when diagonal cracks are produced. One is racking test where a masonry infill panel is subjected to an in-plane racking load. However, the test results are only relevant for this loading condition and wall geometry used in the test. The other two methods are similar in nature. One is diagonal compression test where a compression load is applied onto a masonry wall specimen through steel shoes on two diagonally opposite corners (ASTM E519). This test setup forces cracks to be produced in parallel with the line of action of the compression load. The cracks develop until the wall exhibits a diagonal tension failure in which the specimen splits in the direction parallel to the load applied to it. The other one is often referred to as splitting tension test which is commonly used to gain an understanding of parameters that affect the in-plane tensile strength of masonry.

According to ASTM E519 (2010), the diagonal tensile stress, f_{dt}, obtained using diagonal compression test, is calculated using the following equation:

$$f_{dt} = \frac{0.707P}{A_n} \qquad [2.1]$$

where P is the applied load in N and A_n is the net area in mm^2 calculated as follows:

$$A_n = \left(\frac{w+h}{2}\right)tn \qquad [2.2]$$

where w, h and t are the width, height, thickness of the specimen and n is the percent of the gross area that is solid.

Johnson and Thompson (1969) performed tests on brick masonry disks using the diametral testing procedures. It was found that when the compressive load was normal to the bed joint, the highest tensile strength was observed; whereas the lowest tensile strength was noted when the load was applied parallel to the bed joint.

Drysdale et al. (1979) examined the in-plane tensile strength of grouted and ungrouted concrete masonry assemblages by performing splitting tension tests on 63 full sized specimens. The authors found that minimum capacity was obtained when loading is parallel to the bed joint for ungrouted specimens and maximum capacity was obtained for $\theta = 45$ º for grouted specimens. The authors observed that mortar strength does not contribute significantly to the tensile strength of the assemblage but it only changes the type of failure. On the other hand, filling the cores with grout seemed to significantly increase the tensile strength of the prisms.

Hamid and Abboud (1986) investigated the behavior and strength of 39 quarter-scale grouted and ungrouted concrete block masonry specimens under shear and in-plane tension. The authors examined the tensile strength of the masonry assemblage at different orientations from the bed joint while considering the grout and mortar strength effect on the strength. The authors observed that an increase in tensile strength was evident for ungrouted specimens as the load changed in orientation from being parallel to the bed joints to normal to the bed joints. On the other hand, the authors observed that a slight increase in tensile strength was evident for grouted specimens as the load orientation changed from parallel to 45º but the strength quickly decreased after the load was applied normal to the bed joint.

Mota et al. (2007) and Maleki et al. (2007) performed diagonal tension tests on masonry assemblages to examine the diagonal tensile strength of masonry and the effect of grouting on the strength. All specimens were composed of concrete masonry blocks with type S mortar. Both studies found that grouting increased the diagonal tensile strength significantly. The ultimate strength of hollow specimens was found to be 67% of the strength of the partially grouted specimens and 25% of the strength of fully grouted specimens. The grout in the fully grouted specimens provided continuity that increased the diagonal tensile strength of the infill.

2.2.4 Summary

Previous sections list some important studies on the subject of masonry compressive and shear strength, the following provides a summary of these key findings.

- For prisms loaded in compression normal to the bed face, a minimum of h/t=3 should be considered in order to represent wall behavior. Most researchers found that increasing h/t will lead to a decrease in prism strength. For prisms loaded in compression parallel to the bed face, one researcher commented that h/t ratio does not have an effect on prism strength but unit strength does.
- For both directions of loading, increasing mortar strength increases prism strength. However, most researchers found that this increase is quiet minimal.
- For both directions of loading, ungrouted prisms have higher strength than grouted prisms.
- Prisms loaded normal to the bed joint have a much higher compressive and tensile strength than prisms loaded parallel to the bed joint.
- Most researchers found that mortar strength does not significantly increase the tensile strength but the bond strength of the units and the mortar is a critical parameter to consider.
- Grouting of specimens lead to an increase in the diagonal tensile strength.

Despite that there is a considerable amount of information available on the masonry prism strength, the results presented in all studies were largely scattered and some findings were even contradictory on the effects of various parameters. Majority tests were conducted 40 years ago on the masonry units fabricated then and therefore findings may not be applicable to the masonry units and mortar currently produced in North America. The CSA S304.1 standard committee is in the process of upgrading the specified compressive strength f'_m as well as χ factor to be used in combination with f'_m for loading direction modification. More test results are still in need to augment the existing database and a compilation and analysis of the current and previous results is required to provide recommendations for the standard implementation.

2.3 BEHAVIOR OF MASONRY INFILLED WALLS

In the consideration of masonry strength as affected by the direction of compression, one important application is masonry infills. Masonry infills are commonly used to infill steel or concrete frames. Infill walls interact with the surrounding frame and contribute to the lateral load resistance of the frame system.

The methodology used to consider the infill effect is commonly referred to a "diagonal strut method". This method treats the masonry infilled frame as a braced frame with the masonry infill replaced by an equivalent diagonal strut acting in compression to resist the lateral loading as shown in Figure 2.2. Drysdale and Hamid (2005) described three possible modes of failure of the infills including shear slip failure along the bed joint, diagonal tension shear failure, and compression failure of the diagonal strut which are illustrated in Figure 2.3. All three failures must be evaluated and accounted for in design. However, previous research has shown that for infills of typical geometry and material properties, the failure was predominated by the compression failure of the diagonal strut accompanied with diagonal shear-tension cracking in the infill (Soon, 2011). Compression failure is usually characterized by corner crushing of the masonry between the frame and the masonry infill due to intense stress concentrations at the compressive corners.

Therefore, the accurate evaluation of the ultimate load associated with diagonal compression failure is the important aspect of strength consideration. For the diagonal compression strength evaluation, the stress is assumed to be applied in the direction of the diagonal strut and thus the masonry strength f'_m needs to be modified based on the direction of the stress. Although much research has been dedicated to the stiffness consideration of the infill, the strength of the infills has not been thoroughly examined. The following section provides descriptions of the current code practice for the strength consideration.

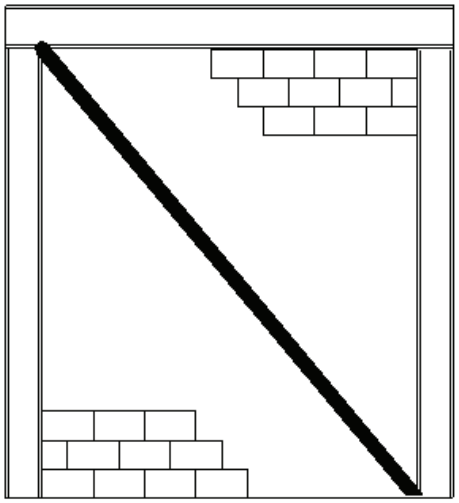

Figure 2.3 Schematic diagram showing the equivalent diagonal strut

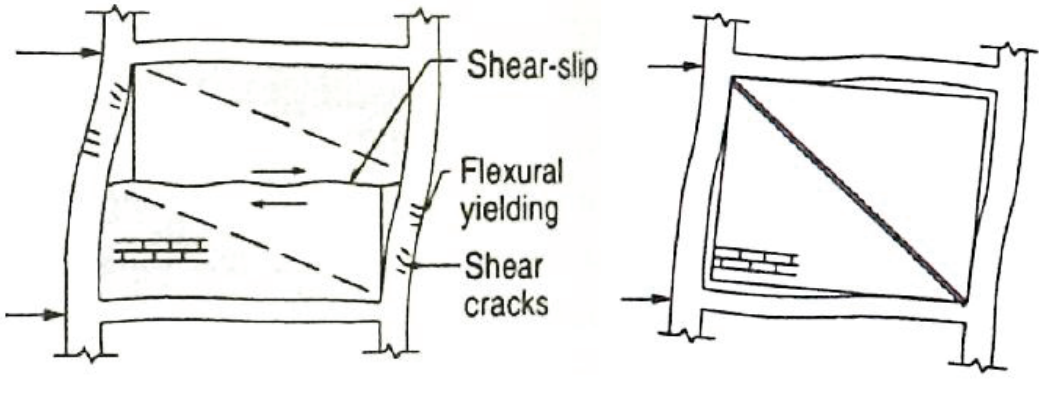

(a) Shear Slip Failure (b) Diagonal Tension Failure

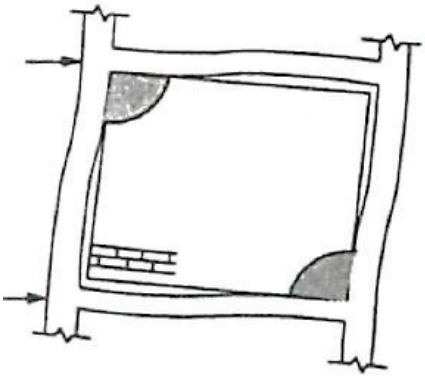

(c) Compression Failure

Figure 2.4 Failure modes exhibited by masonry infill wall (Drysdale and Hamid, 2005)

2.3.1 CSA S304.1-04 and MSJC 2011 Guidelines

CSA S304.1-04 adopts the diagonal strut method and provides provisions for the determination of diagonal strut width. The standard recognizes that the geometric properties of the diagonal strut are a function of the length of contact between the masonry infill and columns, α_h, and between the masonry infill and beams, α_l. Figure 2.4 illustrates the geometric properties of the diagonal compression strut.

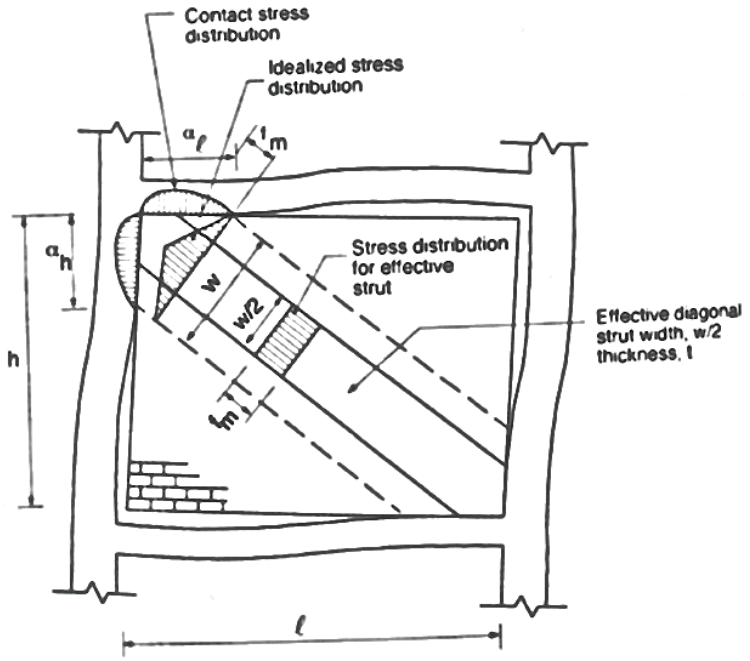

Figure 2.5 Geometric properties of the diagonal compression strut model (Drysdale and Hamid, 2005)

The vertical and horizontal contact lengths α_h and α_l respectively, are calculated as follows:

$$\alpha_h = \frac{\pi}{2}\sqrt[4]{\frac{4E_f I_c h_w}{E_m t_e \sin 2\theta}} \qquad [2.3]$$

$$\alpha_l = \pi\sqrt[4]{\frac{4E_f I_b l_w}{E_m t_e \sin 2\theta}} \qquad [2.4]$$

where E_m is the masonry modulus of elasticity = 850 f'_m, E_f is the modulus of elasticity of the frame, I_c and I_b are the moments of inertia of the column and beam of the frame respectively, h_w, l_w, and t_e are the height, length and effective thickness of the masonry infill respectively, and θ is the angle at which the force acts with the horizontal.

The effective width of the diagonal strut, w_e, can be calculated as

$$w_e = \frac{\sqrt{\alpha_h^2 + \alpha_l^2}}{2} \qquad [2.5]$$

For diagonal compressive strength consideration, CSA S304.1-04 suggests the use of the χ factor to consider the direction of the applied stresses acting on the cross-section. The χ factor is considered to be 0.5 in design. This practice assumes that the compressive strength of the masonry is normal to the head face and this assumption may be highly conservative. The strength equation proposed by the CSA S304.1-04 is essentially the compressive capacity of the diagonal strut modified with χ factor. The proposed equation for calculating the infill ultimate load, V_r, is expressed as follows:

$$V_r = \frac{1}{\sqrt{h_w^2 / l_w^2}} P_r \quad \text{where} \quad P_r = \varphi_m \chi (0.85 f'_m) b(2t_f - r) \quad [2.6]$$

where P_r is the load in the diagonal strut, ϕ_m is the resistance factor for masonry, χ is the factor used to account for direction effect of compressive stress, b is the diagonal strut width, t_f is the flange thickness and r is a solution of a quadratic equation for eccentricity consideration. Furthermore, slenderness effects are to be considered in the design of infill.

The Masonry Standards Joint Committee (2011) also adopted the equivalent diagonal strut method but proposed a different design approach to calculate the diagonal strut width. The width of the diagonal strut, w_{inf}, and the characteristic stiffness parameter, λ_{strut}, are calculated as follows:

$$w_{\inf} = \frac{0.3}{\lambda_{strut} \cos\theta} \qquad [2.7]$$

$$\lambda_{strut} = \sqrt[4]{\frac{E_m t_{net\inf} \sin 2\theta}{4 E_{bc} I_{bc} h_w}} \qquad [2.8]$$

where E_m is the masonry modulus of elasticity = 900 f'_m for concrete masonry and 700 f'_m for clay masonry, E_{bc} is the modulus of elasticity of bounding columns, I_{bc} is the moment of inertia of bounding column for bending in the plane of the infill and t_{netinf} is the net thickness of the infill.

Based on test results obtained by Flanagan and Bennett (2001), MSJC proposed a simple equation for the determination of the corner crushing strength as follows where the diagonal strut width is assumed to be a constant term of 6 inches:

$$(6.0in.) t_{net\inf} f'_m \qquad [2.9]$$

CHAPTER 3 EXPERIMENTAL PROGRAM

3.1 GENERAL

The experimental program is designed to evaluate the behavior and strength of masonry assemblage as affected by several influential parameters. The compressive strengths of masonry normal and parallel to the bed joint are evaluated whereas the splitting tensile strength of masonry is also examined by subjecting the masonry panel to diagonal compressive loading. This chapter is separated into two parts; the testing of prisms and panels and the auxiliary tests for the masonry components, i.e. concrete masonry units, mortar and grout. Prisms are labeled as Series S1 specimens whereas the square panels are labeled as Series S2 specimens.

3.2 TEST SPECIMENS

3.2.1 Series S1 – Prisms

A total of 47 prisms were tested in the evaluation of masonry compressive strength as affected by various parameters. One-third scaled standard blocks were used in the testing. The prisms were tested in accordance with ASTM C1314 (2011). Table 3.1 shows a summary of specimens with various parameters. In the table, the vertical loading direction referred to the situation where the prisms were loaded in compression normal to the bed joint whereas the horizontal loading direction referred to that where the prisms were loaded in compression parallel to the bed joint. Three height-to-thickness ratios (3.28, 4.42, 5.52) were considered where number of courses varied from 3, 4 and 5 blocks high with one block wide as shown in Figure 3.1. Prisms included ungrouted, partially grouted and fully grouted prisms as shown in Figure 3.3. Two mortar types, i.e. Type N and S mortar, were used in the construction of prisms. The mortar was placed on both the face-shell and the web as illustrated in Figure 3.2 as shaded area. The thickness of the mortar joint was reduced to 5 mm for scaled block prisms.

The labeling scheme of Series S1 is explained as follows. The first letter indicates the grouting situation (H, P, or F); the second number represents the number of courses; the third letter indicates the mortar type; and the last letter identifies the loading direction. Specimens with a fifth digit, W, indicates the removal of the central web. For example, S1-H4NV is a hollow 4

block high Type N mortar prism loaded vertically. For both loading direction, the effect of web interruption was investigated using S1- F4NHW and S1- F4SHW where the central web of the blocks was removed and grout was poured continuously without the interruption of the web as shown in Figure 3.4. It is noted that at the beginning of the test program, three identical specimens were tested for a specimen and once the repeatability of the test was established, two specimens were tested. This process was followed throughout the test program.

Table 3.1 Prism specimens for one-third scaled blocks

Specimen ID	Loading Direction	h/t Ratio	Grouting	Mortar Strength	Web Interruption	Number of Specimens
S1–H4NV	Vertical	4.42	Hollow	Type N	Yes	3
S1–P4NV	Vertical	4.42	Partial	Type N	Yes	3
S1–F4NV	Vertical	4.42	Full	Type N	Yes	3
S1–H3NV	Vertical	3.28	Hollow	Type N	Yes	2
S1–F3NV	Vertical	3.28	Full	Type N	Yes	3
S1–H5NV	Vertical	5.52	Hollow	Type N	Yes	2
S1–F5NV	Vertical	5.52	Fully	Type N	Yes	3
S1–H4SV	Vertical	4.42	Hollow	Type S	Yes	2
S1–P4SV	Vertical	4.42	Partial	Type S	Yes	2
S1–F4SV	Vertical	4.42	Fully	Type S	Yes	3
S1–F4SVW	Vertical	4.42	Fully	Type S	No	2
S1–H4NH	Horizontal	–	Hollow	Type N	Yes	3
S1–P4NH	Horizontal	–	Partial	Type N	Yes	2
S1–F4NH	Horizontal	–	Fully	Type N	Yes	3
S1–F4NHW	Horizontal	–	Fully	Type N	No	3
S1–H4SH	Horizontal	–	Hollow	Type S	Yes	2
S1–P4SH	Horizontal	–	Partial	Type S	Yes	2
S1–F4SH	Horizontal	–	Fully	Type S	Yes	2
S1–F4SHW	Horizontal	–	Fully	Type S	Yes	2

(a)

(b)

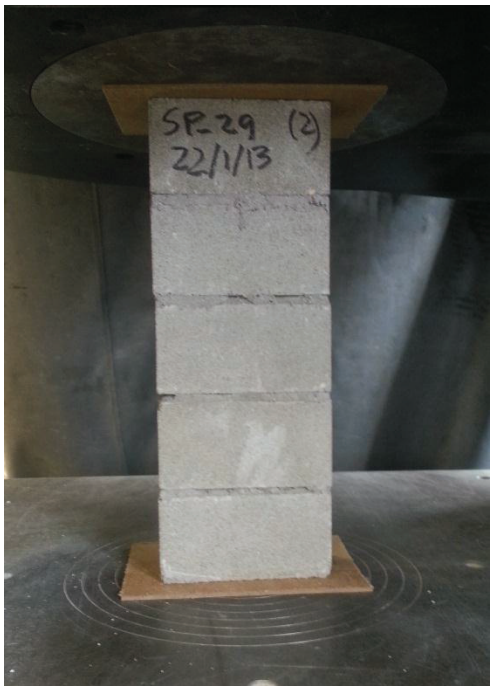

(c)

Figure 3.1 (a) Three, (b) Four and (c) Five-block high prisms

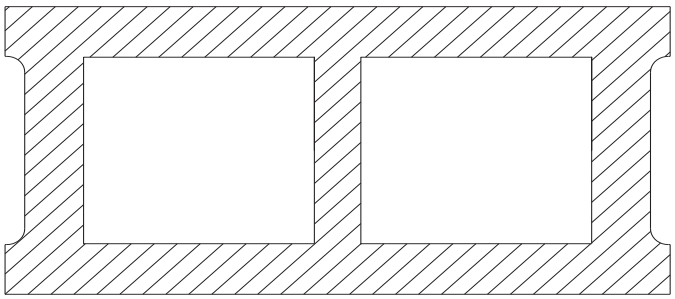

Figure 3.2 Prisms mortar bedding

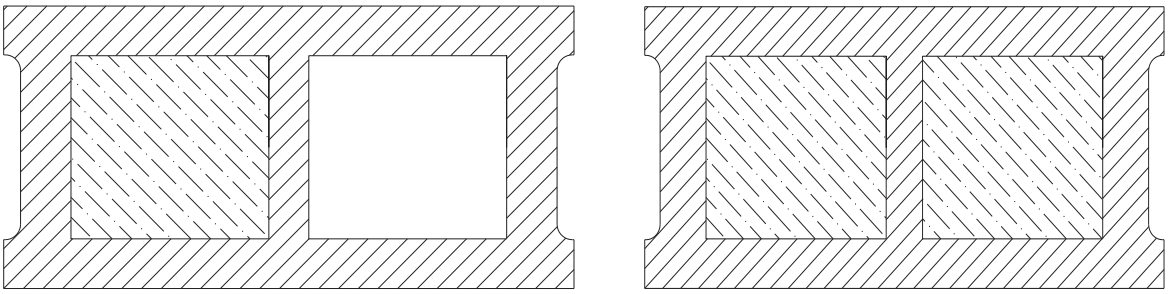

(a) **(b)**

Figure 3.3 (a) Partially grouted and (b) Fully grouted prisms

(a) **(b)**

Figure 3.4 (a) Unit with no central web (b) 4-block high fully grouted prism with no web interruption

3.2.2 Series S2 – Panels

A total of 27 square panels were constructed using one-third scaled blocks. The square panels were loaded in vertical, horizontal and diagonal compression in accordance with ASTM C1314 (2011) and ASTM E519 (2010) as shown in Figure 3.5. Panels under vertical and horizontal loading were tested in a similar procedure to the prisms. As for the panels loaded in the diagonal direction, two custom-made steel loading shoes were placed at the loaded corners to provide a flat surface for the application of the load to the panel. The loading shoe as shown in Figure 3.6 is designed with a V-shaped joint inside a rectangular box.

(a) **(b)**

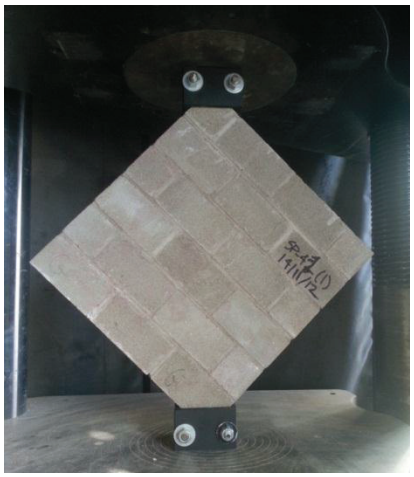

(c)

Figure 3.5 Loading arrangement for square panels under (a) vertical, (b) horizontal and (c) diagonal compression

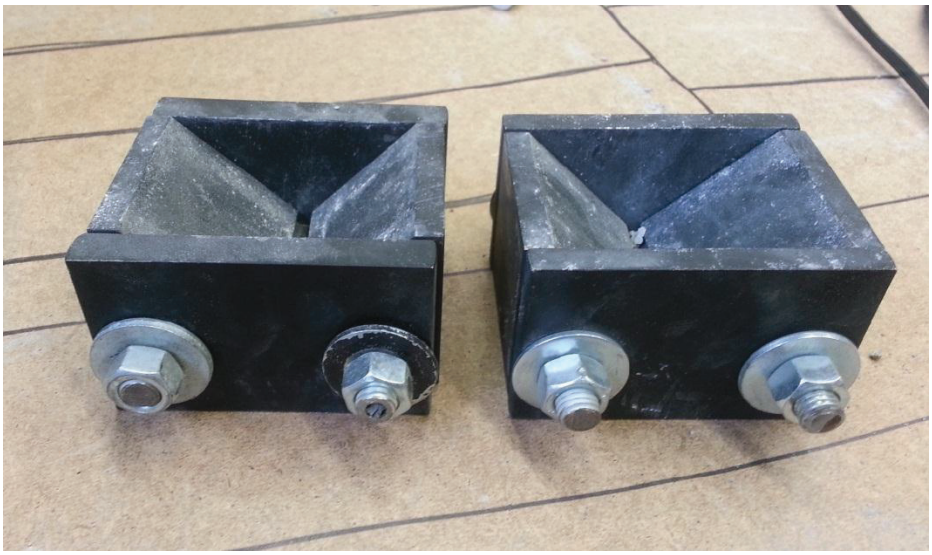

Figure 3.6 Steel loading shoe used in the testing of diagonal panels

The panels were 6 courses high and 3 courses wide as illustrated in Figure 3.7 with a height to thickness ratio of 6.68. Panels are constructed in half running bond where each head joint is positioned at the middle of the unit below it with a joint thickness of 5 mm. Flat end blocks and half blocks are used at the ends; whereas frog-end blocks are used in between. Mortar was applied on the face-shell and the two end webs of the bed joint as shown in Figure 3.8. Mortar was only applied at the face-shell of the head joint. Both Type N and Type S mortar were used. For Type N mortar, seven hollow, seven partially grouted and seven fully grouted panels were fabricated and tested in all three loading orientations. For Type S mortar, two specimens were constructed for each grouting arrangement and tested only under diagonal compression. Figure 3.9 illustrates the grouting configuration of the partially grouted and fully grouted panels. Tables 3.2 show a summary of the specimens.

The labeling scheme of Series S2 is explained as follows. The first letter indicates the grouting situation; the second letter indicates the mortar type; and the last letter identifies the loading direction. For example S2-HNV is a hollow Type N mortar panel vertically loaded.

Table 3.2 Panel specimens for one-third scaled blocks

Specimen ID	Loading Direction	Panel Dimension (m x m)	Grouting	Mortar Strength	Number of Specimens
S2- HNV	Vertical	0.42 x 0.42	Hollow	Type N	3
S2- PNV	Vertical	0.42 x 0.42	Partial	Type N	3
S2- FNV	Vertical	0.42 x 0.42	Full	Type N	3
S2- HNH	Horizontal	0.42 x 0.42	Hollow	Type N	2
S2- PNH	Horizontal	0.42 x 0.42	Partial	Type N	2
S2- FNH	Horizontal	0.42 x 0.42	Full	Type N	2
S2- HND	Diagonal	0.42 x 0.42	Hollow	Type N	2
S2- PND	Diagonal	0.42 x 0.42	Partial	Type N	2
S2- FND	Diagonal	0.42 x 0.42	Partial	Type N	2
S2- HSD	Diagonal	0.42 x 0.42	Hollow	Type S	2
S2- PSD	Diagonal	0.42 x 0.42	Partial	Type S	2
S2- FSD	Diagonal	0.42 x 0.42	Full	Type S	2

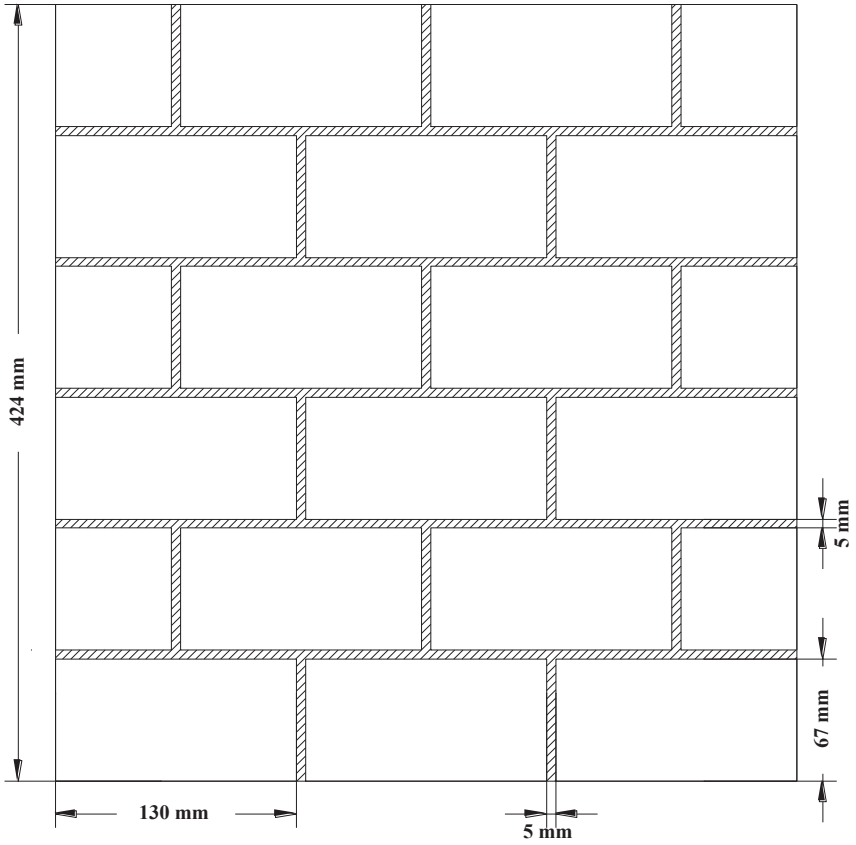

Figure 3.7 Dimensions of square panels

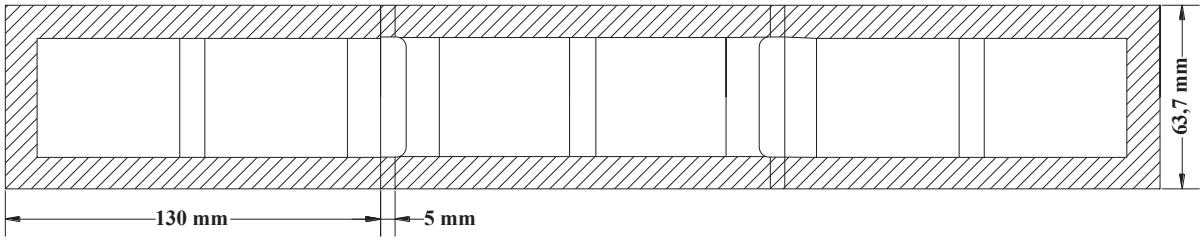

Figure 3.8 Square panels mortar bedding

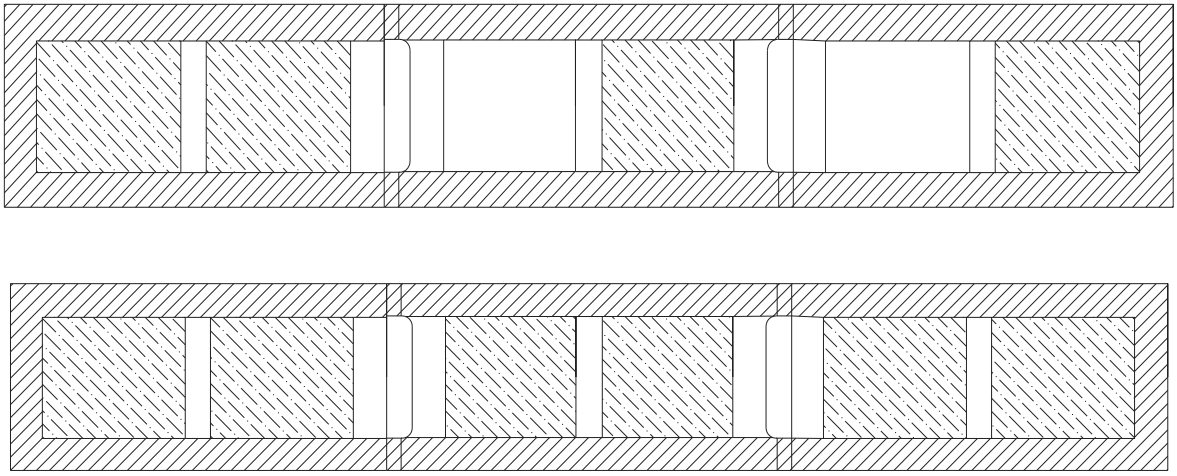

Figure 3.9 Square panels grouting arrangement

3.2.3 Fabrication

All prisms and panels were built to the standard of practice by an experienced mason in the concrete laboratory at the Department of Civil and Recourse Engineering of Dalhousie University. The temperature in the room is around 20ºC and moisture content ranging from 40 to 60%. All specimens were moisture cured under the cover of burlaps which was kept wet for 7 days and then air-cured for at least 28 days till the test date. Concurrent with the prism construction, mortar cubes and grout prisms were cast and cured in accordance with CSA A179 (2004). For both prims and panels, the concrete masonry units were placed carefully and leveled after each course as shown in Figure 3.10. For the panels, mortar was employed on both bed joints and head joints as shown in Figure 3.11. Specimens to be grouted such as those shown in Figure 3.12 where filled with high fluid grout and the grout was manually vibrated inside the cells and compacted to reduce the air pockets to minimum.

Figure 3.10 Leveling the concrete blocks during placement

Figure 3.11 Mortar Placement

Figure 3.12 Specimens with cores filled with grout

3.2.4 Test Procedure

Prior to testing, all loading surfaces of the prisms and panels were scraped and leveled to ensure a smooth contact area. The void between the frog ends of partially grouted and fully grouted prisms under horizontal loading were filled with mortar to ensure a uniform loading. The prisms and panels were tested using the Instron Universal testing machine shown in Figure 3.13. Soft capping, fiberboard, was used to provide a flat bearing surface in order to distribute the load uniformly to the specimen. The specimens were placed on the lower platen of the machine. Both centroidal axes of the specimen were aligned with the center of thrust of the machine. A uniform load of 8,000 N/min was applied to all specimens until the failure of the specimen. Testing was stopped when an irreversible load drop of more than 50% of the maximum load was observed. The load and displacement data were recorded through a built-in data acquisition system in Instron.

Figure 3.13 Instron Universal Testing Machine

3.3 AUXILIARY TESTS

3.3.1 Concrete Masonry Units

One-third scaled concrete masonry units were used in the experimental program. The units evaluated are the frog-end, flat-end and half blocks. Figure 3.14 shows the average dimensions of six frog-end and flat-end blocks for one-third scale blocks. The physical properties of the blocks including percentage absorption, density and moisture content were tested according to ASTM C140 (2012) Standard Test Methods for Sampling and Testing Concrete Masonry Units and Related Units. The compressive strength of the concrete masonry units was also tested according to ASTM C140 (2012).

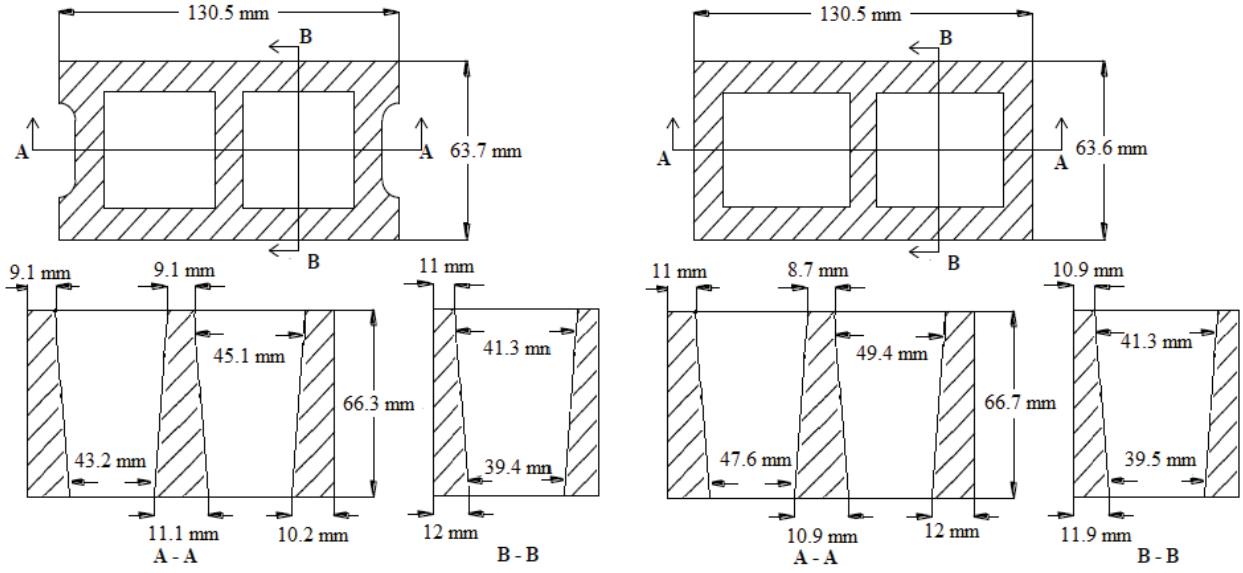

(a) **(b)**

Figure 3.14 Dimensions of one-third scale units: (a) frog-end, (b) flat-end block

3.3.2 Mortar

Two types of mortar, Type S and N, were used in the experimental program. The composition of mortar included either Type S or Type N masonry cement and sand with the same respective ratio of 1:3. The construction and testing of mortar cubes was according to CSA A179 (2004) Mortar and Grout for Unit Masonry. Three 50 mm (2 inch) mortar cubes for each prism were prepared in a non-absorbent molds as the mortar was being mixed on site as shown in Figure 3.15. The mortar cubes were cured for seven days in the moisture room with two days being cured in their molds. The mortar cubes were either tested for compressive strength at seven days or twenty-eight days. The mortar cubes to be tested at twenty-eight days were taken out of the moisture room after seven days and placed in lime water for further curing until the test date as shown in Figure 3.16.

Figure 3.15 Mortar cubes in mold

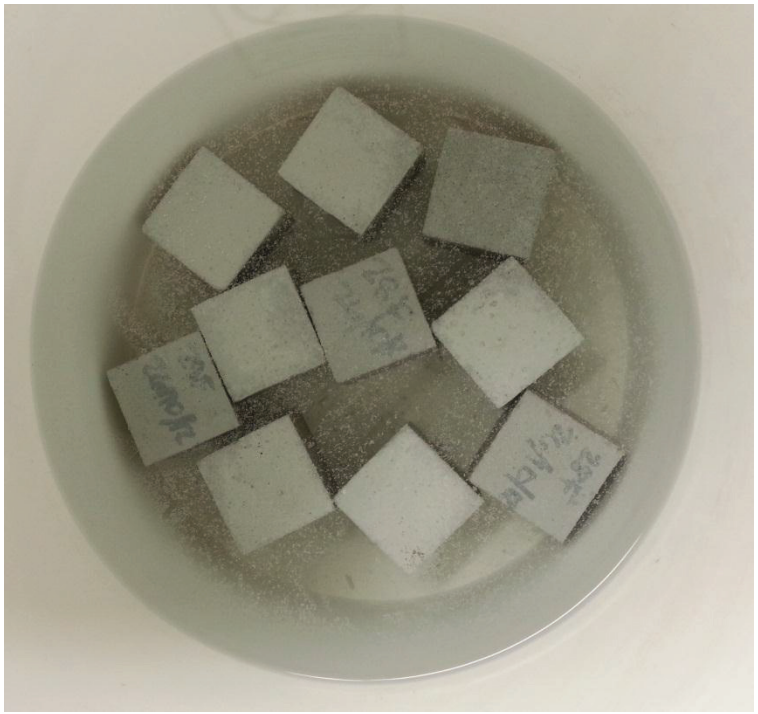

Figure 3.16 Mortar cubes placed in lime-water

3.3.3 Grout

The dry mix of the grout was composed of Type S or N masonry cement and sand with a respective ratio of 1:3. A sufficient amount of water is added in order to achieve the fluidity of the grout and a slump in the range of 200-250 mm according to CSA A179 (2004). The grout mix was poured into a mold composed of four unit blocks as shown in Figure 3.17 in order to represent the effect of water absorbed in actual construction. Paper towel is used to line the mold to facilitate de-molding of these grout specimens. Three cube molds were done for each batch of grout and were left in the mold to be air-cured for two days then taken out and cured in the moisture room until the test date in accordance with CSA A179 (2004). Testing of the compressive strength of the grout was done at twenty-eight days.

Figure 3.17 Grout cubes in mold

CHAPTER 4 EXPERIMENTAL RESULTS AND DISCUSSION

4.1 INTRODUCTION

The results of the masonry components, prisms and panel specimens are presented. The masonry component results include the physical and mechanical properties of concrete masonry unit, mortar and grout. The results of prisms and panel specimens focus on the behavior of these specimens under compressive loading as affected by various parameters including load direction, height-to-thickness ratio, mortar strength and grouting situation.

4.2 MASONRY COMPONENT RESULTS

4.2.1 Physical Properties

Three frog-end and three flat-end full size blocks were randomly selected and tested for absorption, moisture content and density in accordance with ASTM C140 (2012). The received weight of each unit was first measured and then the blocks were immersed in water for 24 hours. As the blocks were submerged in water, they were weighted and the immersed weight was obtained. After removal from the water, the weight of the block was measured to attain the saturated weight. The blocks were then dried in the oven at approximately 105°C for 24 hours and the oven-dry weight was subsequently recorded.

Table 4.1 presents the results obtained for absorption, moisture content and density as well as their respective average, standard deviation and coefficient of variation (COV) for the frog-end (FR) and flat-end units (FL), respectively. For the frog-end units, the average absorption obtained was 159.3 kg/m^3 with a COV of 6.8%; the average moisture content was 14.9% with a COV of 8.1%; the average density was 2058.9 kg/m^3 with a COV of 1.3%. For the flat-end units, the average absorption obtained was 172.7 kg/m^3 with a COV of 3.7%; the average moisture content was14.5% with a COV of 3.1%; the average density was 2033.8 kg/m^3 with a COV of 0.3%. The low COV values in all cases indicate that the block units used in this study have consistent physical properties. According to CAN/CSA A165-04 (2009), a standard 200 mm hollow block shall have a density greater than 2000 kg/m^3, absorption of less than 175 kg/m^3 and maximum moisture content of 45% for a relative humidity higher than 75%. The average

results for both the frog-end units and flat-end units are well within the range of the specifications required.

Table 4.1 Physical properties of one-third scaled concrete masonry units

ID	Received Weight (g)	Immersed Weight (g)	Saturated Weight (g)	Dry Weight (g)	Absorption (kg/m^3)	Absorption (%)	Moisture Content (%)	Density (kg/m^3)
FR-1	574	335.6	615	567	171.8	8.5	14.6	2029.3
FR-2	592	347.2	628	585	153.1	7.4	16.3	2083.3
FR-3	586	342.0	623	580	153.0	7.4	14.0	2064.1
				Avg.	159.3	7.7	14.9	2058.9
				Std. Dev.	10.8	0.6	1.2	27.4
				COV (%)	6.8	8.1	8.1	1.3
FL-1	574	337.2	617	567	178.7	8.8	14.0	2026.4
FL-2	584	341.0	624	577	166.1	8.1	14.9	2038.9
FL-3	571	335.0	612	564	173.3	8.5	14.6	2036.1
				Avg.	172.7	8.5	14.5	2033.8
				Std. Dev.	6.3	0.3	0.5	6.5
				COV (%)	3.7	4.0	3.1	0.3

4.2.2 Mechanical Properties

The compressive strength of concrete masonry units was determined according to ASTM C140 whereas the compressive strengths of mortar and grout were determined according to CSA A179 (2004).

4.2.2.1 Concrete Masonry Units

Three frog-end and 3 flat-end units were randomly selected and tested in compression using the Instron Universal testing machine. The block surface dimensions were measured using a digital caliper. The blocks were capped using fiberboard to ensure uniform loading. Table 4.2 presents the compressive strength of the frog-end (FR) and flat-end units (FL). The compressive strength was calculated by dividing the ultimate load by the net area of the unit. The average compressive

strength obtained for the frog-end units was 19.3 MPa with a COV of 6.2%. For the flat-end units, the average compressive strength was 14.1 MPa with a COV of 11.3%. The COV value was less than 15% for both unit geometries, which is considered acceptable.

Table 4.2 Compressive strength of one-third scaled concrete masonry units

ID	Area (mm^2)	Ultimate Load (kN)	Compressive Strength (MPa)
FR-4	4122.46	81.4	19.7
FR-5	4106.97	74.2	18.1
FR-6	4110.10	82.3	20.0
		Avg.	19.3
		Std Dev.	1.2
		COV(%)	6.2
FL-4	4244.53	52.6	12.4
FL-5	4251.10	62.0	14.6
FL-6	4238.67	65.1	15.4
		Avg.	14.1
		Std Dev.	1.6
		COV(%)	11.3

Figure 4.1 and Figure 4.2 show the typical failure mode of the frog-end and flat-end units under compression, respectively. The typical failure mode was conical shear failure for both block geometries.

(a) FR-4: Conical Shear Failure **(b) FR-5: Conical Shear Failure**

Figure 4.1 Failure of frog-end units under compression

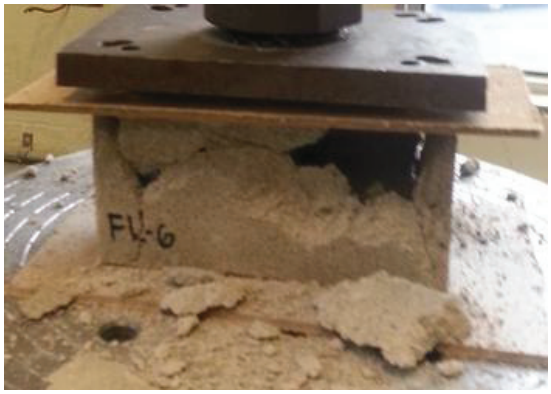

(c)FL-5: Conical Shear Failure **(d) FL-6: Conical Shear Failure**

Figure 4.2 Failure of flat-end units under compression

4.2.2.2 Mortar

Two types of mortars, Type S and Type N, were used in the construction of both prisms and panels. The composition of mortar included either Type S or Type N masonry cement and sand with a volumetric ratio of 1:3. Several batches of mortar were mixed and mortar cubes were made from each batch relative to the specimen it was constructed for. A total of sixty-three 50 mm mortar cubes were tested, twelve of which were tested for their 7-day strength and fifty-one were tested for their 28-day strength according to CSA A179 (2004). Figure 4.3 shows the typical failure of mortar cubes under compressive loading. A form of conical shear failure was observed for both mortar types.

Figure 4.3 Failure of mortar cubes under compression

The compressive strength for Type N mortar cubes are summarized in Table 4.3 for 28-day compressive strength. The "Mean Compressive Strength" column shows the average of the compressive strength values for each batch and the number in the bracket indicates the number of cubes tested. The mean 28-day compressive strength of all Type N mortar cubes is found to be 5.1 MPa. The COV values for all batches are below the 15% limit. The mean compressive strength for Type N mortar is above the minimum limit of 5.0 MPa specified in CSA A179 (2004) for laboratory prepared mortar cubes.

Table 4.3 The 28-day mean compressive strength of Type N mortar cubes

Batch Number	Mean Compressive Strength (MPa)	COV (%)
1	5.2 (3)	1.7
2	5.6 (3)	0.8
3	5.6 (3)	1.3
4	5.8 (3)	3.3
5	5.3 (3)	2.2
6	3.8 (6)	9.0
7	5.5 (6)	5.6
8	4.0 (6)	2.4

The 28-day compressive strength for Type S mortar cubes are summarized in Table 4.4. The mean compressive strength for all Type S mortar cubes was found to be 7.1 MPa. This value is lower than the minimum limit of 12.5 MPa specified in CSA A179 (2004). However, the low COV values (< 15%) suggested that strengths for all batches were consistent. Considering that the objective of having two different mortar strengths was achieved, these mortar batches were kept and used in the construction.

Table 4.4 The 28-day mean compressive strength of Type S mortar cubes

Batch Number	Mean Compressive Strength (MPa)	COV (%)
1	8.6 (3)	0.9
2	6.5 (6)	11.5
3	6.7 (3)	10.5
4	6.5 (6)	11.1

4.2.2.3 Grout

Grout was mixed from both Type S or Type N masonry cement and sand with a sufficient amount of water added to the composition. A total of twenty-seven grout cubes were tested for their 28-day strength according to CSA A179 (2004). Figure 4.4 shows the typical failure of grout cubes under compressive loading which was indicated as a vertical cracking failure.

Figure 4.4 Failure of grout cubes under compression

The 28-day compressive strength for Type N and Type S grout cubes are summarized in Table 4.5 and Table 4.6, respectively. The batch number in Table 4.5 and Table 4.6 corresponds to the mortar batch number in Table 4.3 and Table 4.4, respectively. The mean 28-day compressive strengths of Type N and Type S grout cubes were found to be 5.5 MPa and 6.8 MPa, respectively. The COV values for all batches of grout strength are below the 15% limit with the exception of batch 3 for Type S grout which has a COV value of 16.9%.

Table 4.5 The 28-day Mean compressive strength of Type N grout cubes

Batch Number	Mean Compressive Strength (MPa)	COV (%)
2	5.6 (3)	2.2
3	5.6 (3)	4.5
4	6.3 (3)	5.6
5	5.7 (3)	3.2
6	4.6 (3)	4.0
7	5.0 (3)	12.1

Table 4.6 The 28-day Mean compressive strength of Type S grout cubes

Batch Number	Mean Compressive Strength (MPa)	COV (%)
1	8.6 (3)	3.1
2	5.4 (3)	10.5
3	6.5 (3)	16.9

4.2.2.4 Summary of Auxiliary Tests

The overall mean compressive strengths obtained for the frog-end units and flat-end units were 19.3 MPa and 14.1 MPa, respectively. The overall mean 28-day compressive strengths for Type N and Type S mortar were 5.1 MPa and 7.1 MPa, respectively. The overall mean 28-day compressive strengths for Type N and Type S grout were 5.5 MPa and 6.8 MPa, respectively.

4.3 SPECIMEN RESULTS– COMPRESSIVE STRENGTH

4.3.1 Ultimate Load

For the study of masonry compressive strength, series S1 specimens included 47 prisms in 19 groups and series S2 specimens included 15 square panels in 6 groups. Each group represents a combination of parameters being studied. The parameters included in the study are loading direction, mortar strength, height-to-thickness ratio, and grouting situation. Prisms and panels loaded either vertically or horizontally were tested in accordance with ASTM C1314 (2011).

The effective area used in the strength calculation is defined in the following. For prisms loaded in compression normal to the bed joint, the shaded area shown in Figure 4.5 is used for hollow, partially grouted and fully grouted specimens. The net area for hollow, partially grouted and fully grouted specimens is calculated to be 4,113 mm^2, 5,926 mm^2 and 7,770 mm^2, respectively.

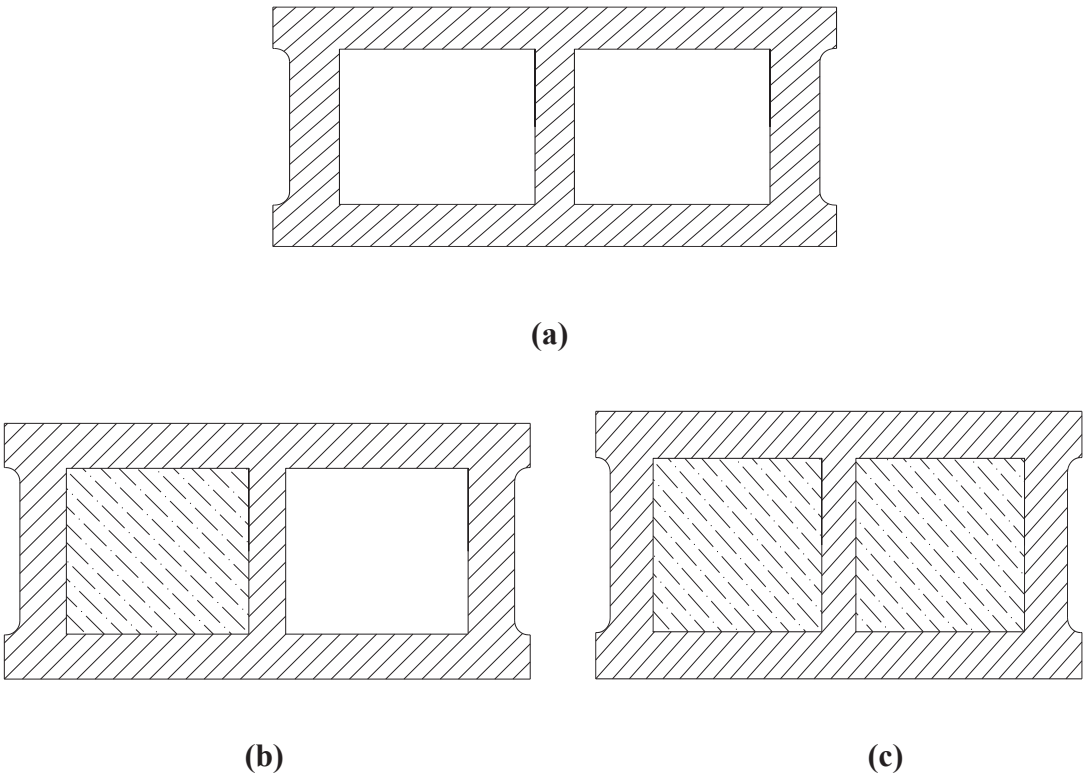

(a)

(b) **(c)**

Figure 4.5 Effective area for (a) hollow, (b) partially grouted and (c) fully grouted prisms

For prisms loaded in compression parallel to the bed joint, the net area for hollow and partially grouted is the face-shell area with the addition of the mortar joint thickness as shown in Figure 4.6 and is calculated to be 6,343 mm^2. It is noted that the grouted core is not included in the net area calculation since the grouting is not continuous to the bearing surface when the prism is loaded horizontally. The net area for fully grouted prisms is the gross cross-sectional area as shown in Figure 4.7 and is calculated to be 17,712 mm^2.

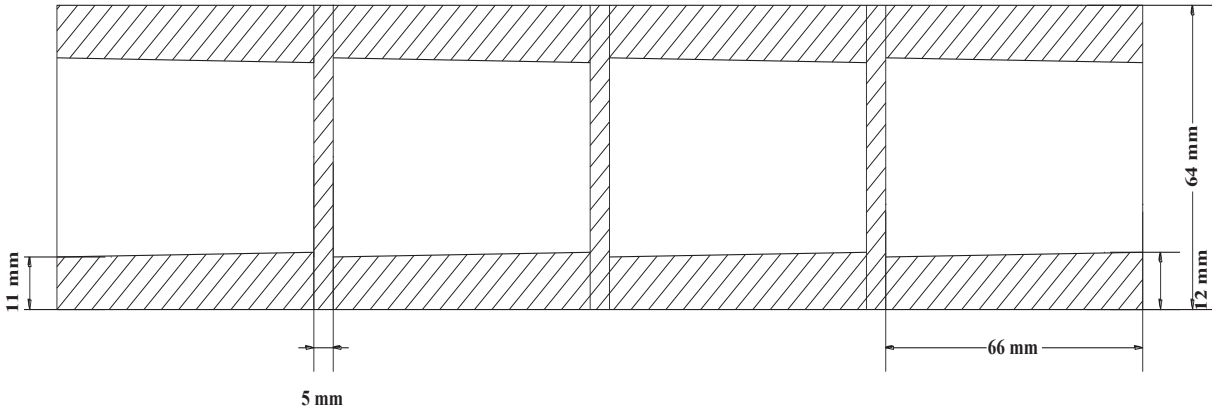

Figure 4.6 Net area of hollow and partially-grouted prisms loaded parallel to the bed joint

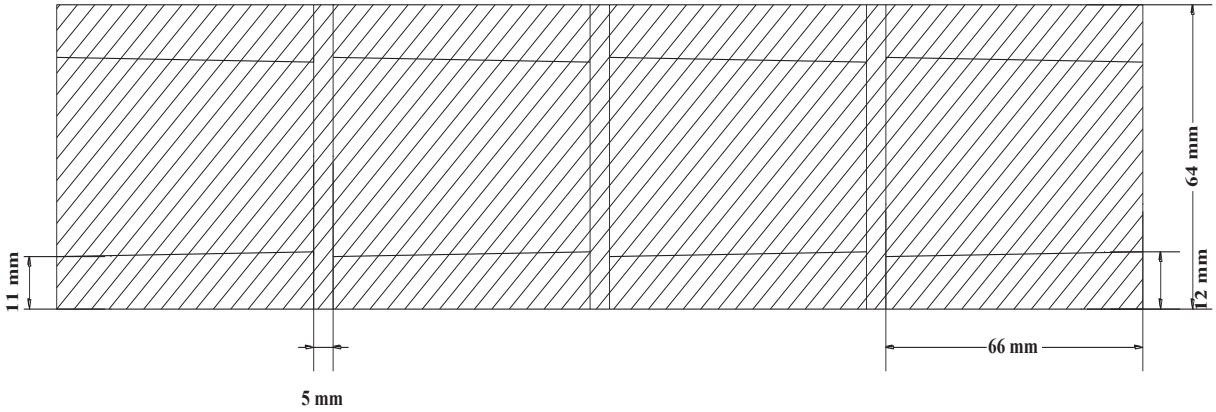

Figure 4.7 Net area of fully-grouted prisms loaded parallel to the bed joint

For panels loaded either vertically or horizontally, the net areas for hollow, partially and fully grouted specimens are defined as the shaded areas in Figure 4.8. The net area for hollow, partially grouted and fully grouted panels is 9,439 mm^2, 17,131 mm^2 and 20,888 mm^2, respectively. It is noteaverad that effective net area (shaded area) includes only mortar bedded flange/web areas and grouted filled cell areas for partially and fully grouted panels.

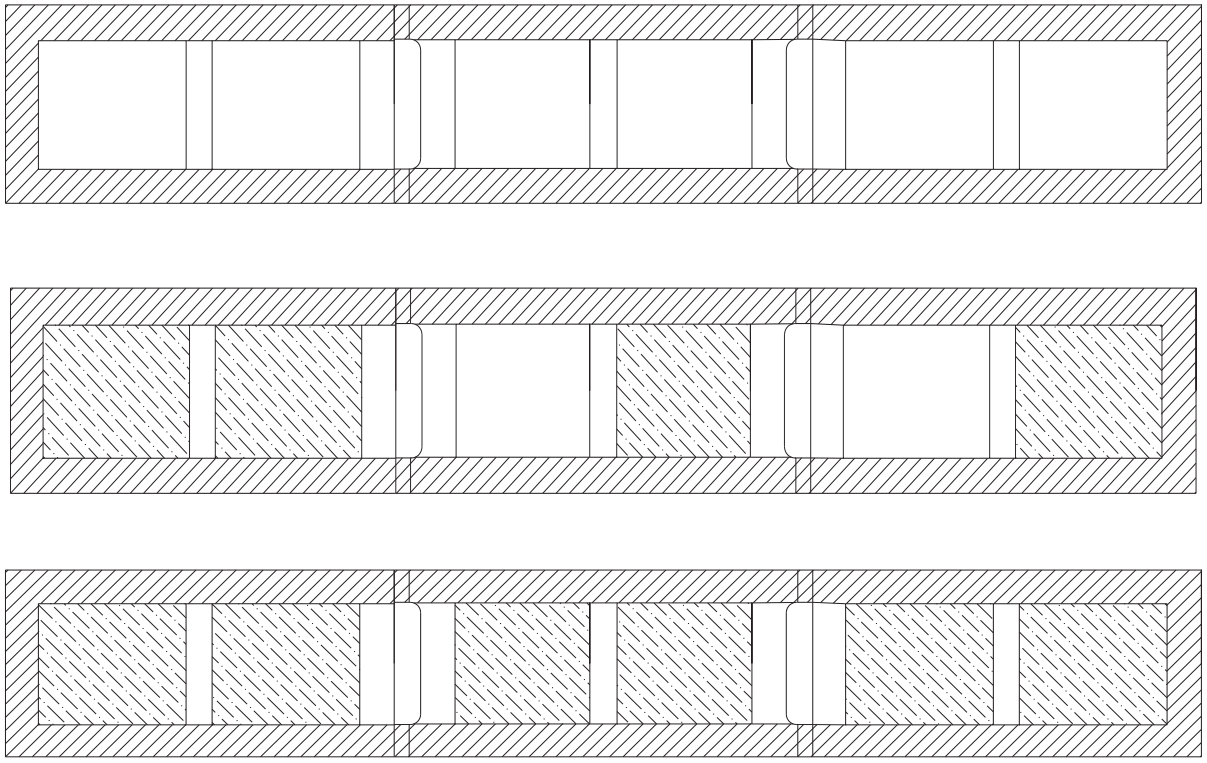

Figure 4.8 Net area of hollow, partially grouted and fully grouted panels

The mean ultimate load for specimens tested in each group is shown in Table 4.7. The number of specimens tested in that group is shown in the bracket. It is noted that COV values of groups having 3 specimens were within the 15% specified limit, indicating that the test specimens and set up have achieved the repeatability. Therefore, for some groups, only 2 specimens were tested.

Table 4.7 Mean compressive strength of prisms and panels

Specimen ID	Loading Orientation	Grouting	Mortar Strength (MPa)	Ultimate Load (N)	Mean Compressive Strength (MPa)	COV (%)
S1–H4NV	Vertical	Hollow	3.8	32,112	7.8 (3)	11.2
S1–P4NV	Vertical	Partially	3.8	40,762	6.9 (3)	15.0
S1–F4NV	Vertical	Fully	5.8	51,261	6.6 (3)	4.8
S1–H3NV	Vertical	Hollow	3.8	34,138	8.3 (2)	–
S1–F3NV	Vertical	Fully	5.6	53,192	6.9 (3)	9.8
S1–H5NV	Vertical	Hollow	3.8	38,150	9.3 (2)	–
S1–F5NV	Vertical	Fully	5.6	60,837	7.8 (3)	12.7
S1–H4SV	Vertical	Hollow	6.5	40,014	9.7 (2)	–
S1–P4SV	Vertical	Partially	8.6	50,376	8.5 (2)	–
S1–F4SV	Vertical	Fully	8.6	59,939	7.7 (3)	14.3
S1–F4SVW	Vertical	Fully	6.7	50,013	6.4 (2)	–
S1–H4NH	Horizontal	Hollow	5.2	67,005	10.6 (3)	12.5
S1–P4NH	Horizontal	Partially	5.6	58,539	9.2 (2)	–
S1– F4NH	Horizontal	Fully	5.3	127,884	7.2 (3)	7.6
S1-F4NHW	Horizontal	Fully	5.3	104,501	5.9 (3)	5.0
S1– H4SH	Horizontal	Hollow	8.6	74,232	11.7 (2)	–
S1– P4SH	Horizontal	Partially	8.6	74,110	11.7 (2)	–
S1– F4SH	Horizontal	Fully	8.6	143,540	8.1 (2)	–
S1– F4SHW	Horizontal	Fully	6.7	67,306	3.8 (2)	–
S2–HNV	Vertical	Hollow	4.0	49,780	5.3 (3)	10.0
S2–PNV	Vertical	Partially	4.0	67,790	4.0 (3)	9.0
S2–FNV	Vertical	Fully	4.0	65,860	3.2 (3)	5.6
S2–HNH	Horizontal	Hollow	4.0	48,940	5.2 (2)	–
S2–PNH	Horizontal	Partially	4.0	59,114	3.5 (2)	–
S2–FNH	Horizontal	Fully	4.0	62,664	3.0 (2)	–

4.3.2 Parametric Study

4.3.2.1 Loading Direction

Table 4.8 provides the mean compressive strength of vertically and horizontally loaded prisms for different grouting arrangement and mortar strength used for determining the effect of loading direction.

Table 4.8 Mean compressive strength of prisms for loading direction comparison

Specimen ID	Loading Orientation	Grouting	Mortar Strength (MPa)	Ultimate Load (N)	Mean Compressive Strength (MPa)	COV (%)
S1–H4NV	Vertical	Hollow	3.8	32,112	7.8 (3)	11.2
S1–H4NH	Horizontal	Hollow	5.2	67,005	10.6 (3)	12.5
S1–P4NV	Vertical	Partially	3.8	40,762	6.9 (3)	15.0
S1–P4NH	Horizontal	Partially	5.6	58,539	9.2 (2)	–
S1–F4NV	Vertical	Fully	5.8	51,261	6.6 (3)	4.8
S1– F4NH	Horizontal	Fully	5.3	127,884	7.2 (3)	7.6
S1–H4SV	Vertical	Hollow	6.5	40,014	9.7 (2)	–
S1– H4SH	Horizontal	Hollow	8.6	74,232	11.7 (2)	–
S1–P4SV	Vertical	Partially	8.6	50,376	8.5 (2)	–
S1– P4SH	Horizontal	Partially	8.6	74,110	11.7 (2)	–
S1–F4SV	Vertical	Fully	8.6	59,939	7.7 (3)	14.3
S1– F4SH	Horizontal	Fully	8.6	143,540	8.1 (2)	–
S1–F4SVW	Vertical	Fully	6.7	50,013	6.4 (2)	–
S1– F4SHW	Horizontal	Fully	6.7	67,306	3.8 (2)	–

Figure 4.9 illustrates the effect of loading direction on the compressive strength of the 4-high prisms listed in Table 4.7. Except for specimen S1-F4SW which is fully grouted and with no central web, prisms loaded parallel to the bed joint were found to exhibit higher strength than prisms loaded normal to the bed joint for all grouting configurations and mortar strengths considered. For example, partially grouted prisms loaded horizontally had a 36% increase in strength when compared to similar prisms loaded vertically. Horizontally loaded hollow prisms

attained approximately 28% higher strength than their vertically loaded counterparts whereas fully grouted prisms showed approximately 12% higher strength than similar prisms loaded vertically. Excluding S1-F4SW, the average horizontal-to-vertical strength ratio was determined to be 1.5.

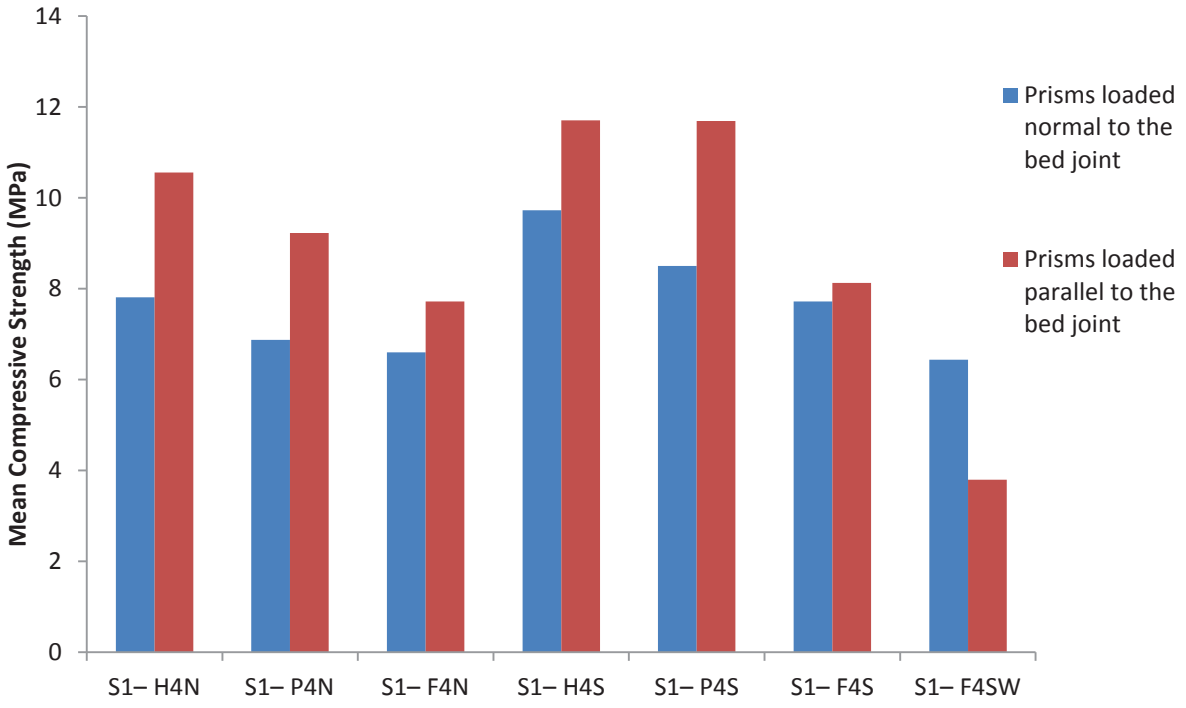

Figure 4.9 The effect of loading direction on compressive strength of prisms

Vertically loaded hollow prisms exhibited face-shell spalling and vertical crack through the web and face-shell as can be seen in Figure 4.10. Partially grouted and fully grouted prisms exhibited similar failure modes as hollow prisms while the grouted column remained intact as shown in Figure 4.11 and Figure 4.12. Same failure modes were found for both Type S and Type N prisms.

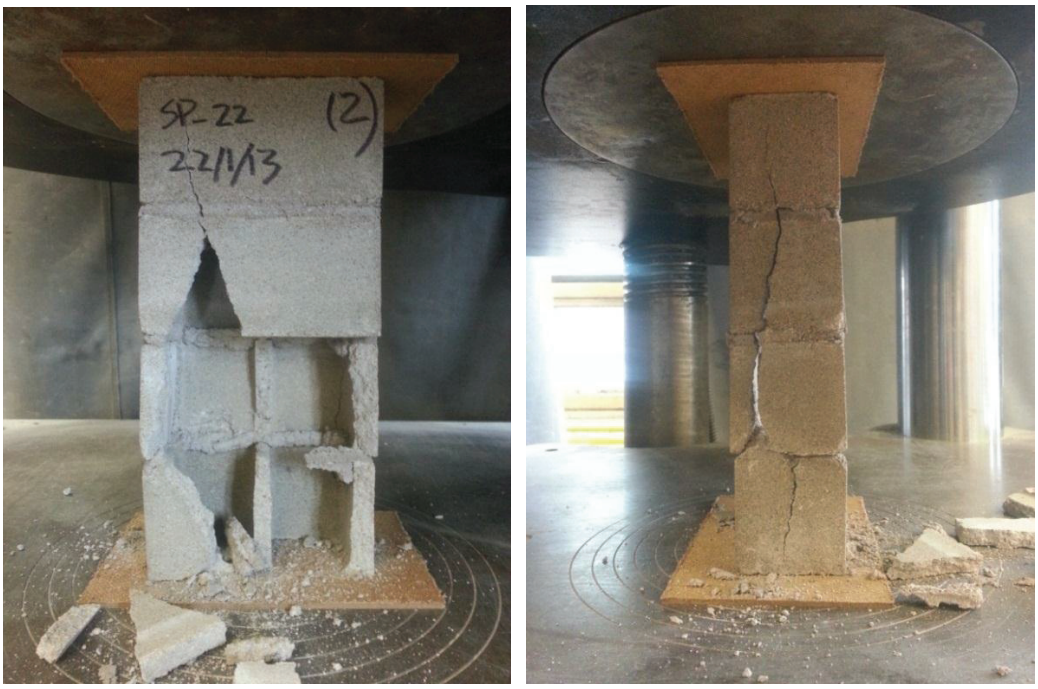

Face-Shell spalling and Vertical crack Vertical crack (web)

Figure 4.10 Failure mode of specimen S1-H4NV

Figure 4.11 Failure mode of specimen S1-P4NV

Figure 4.12 Failure mode of specimen S1-F4NV

For horizontally loaded prisms, while vertical cracking through face-shell and face-shell spalling were also observed, diagonal cracking through face-shell was pronounced as shown in Figure 4.13 and Figure 4.14. Similar to vertically loaded prisms, the grouted column remained intact after failure as shown in Figure 4.15.

Vertical Crack (face-shell)

Figure 4.13Failure mode of specimen S1-H4NH

Figure 4.14 Failure mode of specimen S1-P4NH

Figure 4.15 Failure mode of specimen S1-F4NH

For the case of specimens S1-F4SW, prisms with no central web, the prisms loaded normal to the bed joint were found to have 68% higher strength than those loaded parallel to the bed joint. The failure modes of S1-F4SW are shown in Figure 4.16 for the vertically loaded prism and in Figure 4.17 for the horizontally loaded prism. The failure of the vertically loaded prism with no central web (S1-F4SVW) exhibited vertical cracking through the web and face-shell spalling but with the grouted column remaining fully intact. The horizontally loaded prism with no central web (S1-F4SHW) showed a premature failure initiated by the crushing and longitudinal cracking at the bottom of the prism. This may have attributed to the low ultimate strength observed in this specimen.

Figure 4.16 Failure mode of specimen S1-F4SVW

Figure 4.17 Failure mode of specimen S1-F4SHW

The effects of loading direction on prism compressive strength is further illustrated in stress-strain curves shown in Figure 4.18, Figure 4.19 and Figure 4.20 for hollow, partially grouted and fully grouted prisms, respectively.

As seen in the figures, the prisms loaded horizontally showed a lower initial stiffness and reached a higher strain at the ultimate load than those loaded vertically. However, the overall behavior was similar between the two loading direction where the response remained practically linear up to 80 to 90% of the ultimate load.

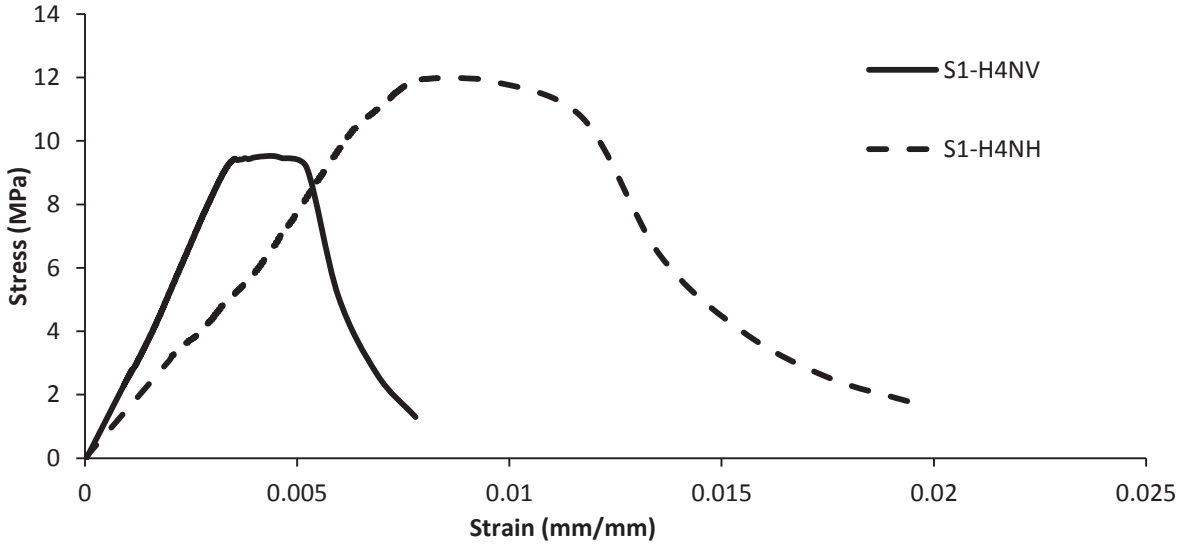

Figure 4.18 Stress-strain curve on the effects of loading direction on hollow prisms

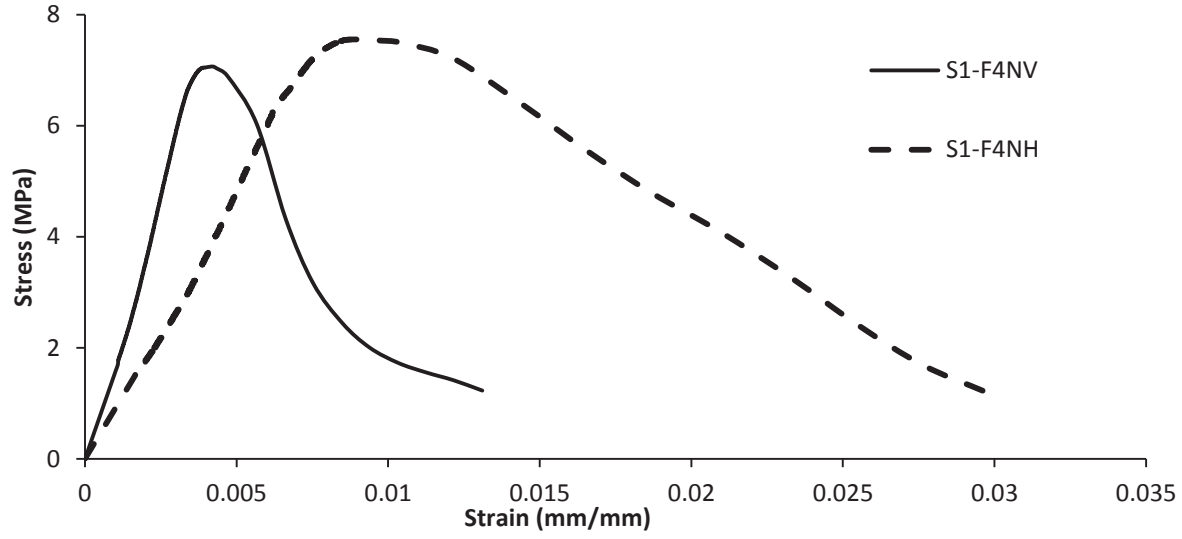

Figure 4.19 Stress-strain curve on the effects of loading direction on partially grouted prisms

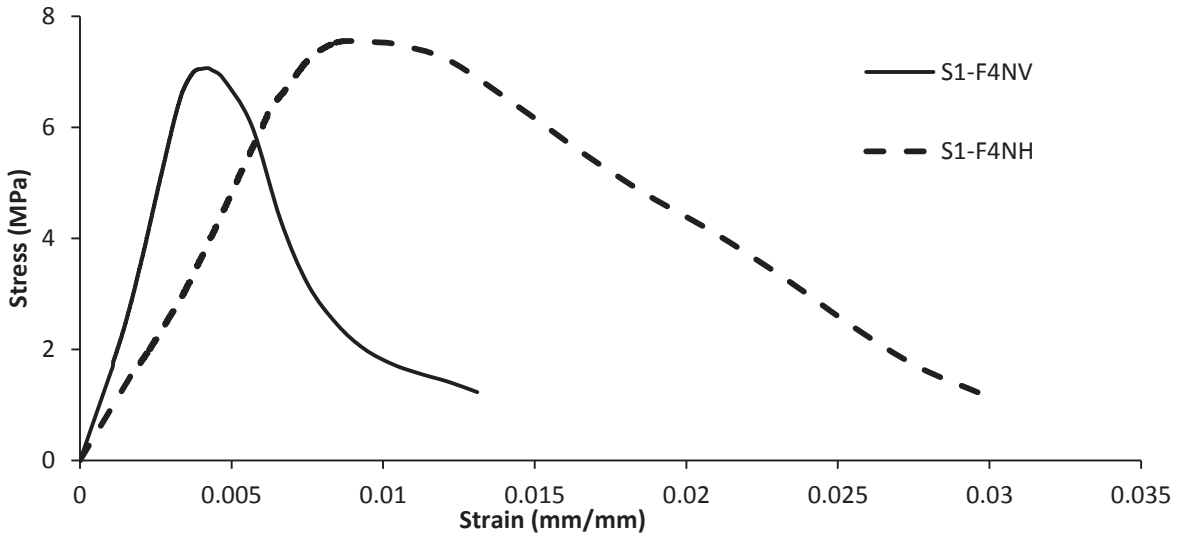

Figure 4.20 Stress-strain curve on the effects of loading direction on fully grouted panels

The observation of compressive strength of prisms loaded horizontally being higher than that of prisms loaded vertically is surprising since the current standard suggest that the compressive strength parallel to the bed joint is much weaker than that normal to the bed joint. It is thought that the high strength observed for horizontally loaded specimens in this study might be attributed to the confinement effect. Since the loading surfaces of the compression machine are very stiff and the size of the specimen is small, this may exert bi-axial compression on the masonry which results in higher strengths.

To minimize the confinement effect, panel specimens were also tested under compression either parallel or vertical to the bed joints. Panel specimens incorporated more mortar joints in running bond thus representing the actual configuration of the masonry assemblage in construction. It is also noted that the effective areas used for the calculation for panel specimens are the same for both loading directions, which eliminates the discrepancy resulted from the use of different area in the calculation of strength. Table 4.9 provides the mean compressive strength of vertically and horizontally loaded panels for different grouting arrangement used for determining the effect of loading direction.

Table 4.9 Mean compressive strength of panels for loading direction comparison

Specimen ID	Loading Orientation	Grouting	Mortar Strength (MPa)	Ultimate Load (N)	Mean Compressive Strength (MPa)	COV (%)
S2–HNV	Vertical	Hollow	4.0	49,780	5.3 (3)	10.0
S2–HNH	Horizontal	Hollow	4.0	48,940	5.2 (2)	–
S2–PNV	Vertical	Partially	4.0	67,790	4.0 (3)	9.0
S2–PNH	Horizontal	Partially	4.0	59,114	3.5 (2)	–
S2–FNV	Vertical	Fully	4.0	65,860	3.2 (3)	5.6
S2–FNH	Horizontal	Fully	4.0	62,664	3.0 (2)	–

The effect of loading direction on the compressive strength of panels is illustrated in Figure 4.21. Vertically loaded panels showed small increases in strength when compared to similar panels loaded horizontally; a 1%, 15% and 1% increase for hollow, partially grouted and fully grouted panels respectively. The average horizontal-to-vertical strength for panel specimens was determined to be 0.94. While more testing is required to provide conclusive findings, it is felt that specimen incorporating a running bond construction such as panel specimens used in this study should be used for conducting strength comparison for loading directions.

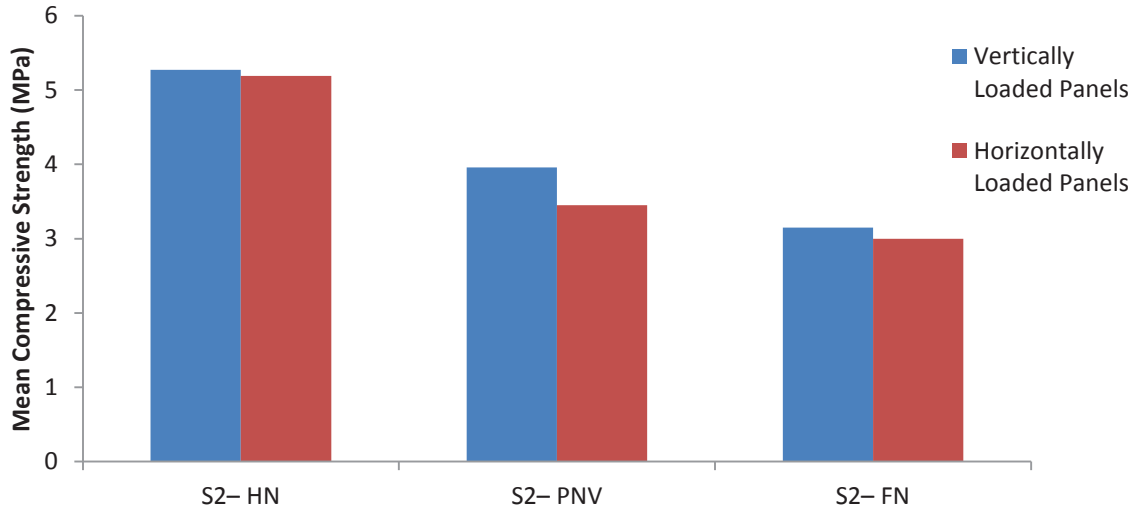

Figure 4.21 The effect of loading direction on compressive strength of panels

The panel failure modes are discussed in the following. The vertically loaded panels exhibited similar failure modes as vertically loaded prisms where face-shell spalling and vertical cracking through the face-shell were observed as shown in Figures 4.22 to 4.24.

Figure 4.22 Failure mode of specimen S2- HNV

Figure 4.23 Failure mode of specimen S2- PNV

Figure 4.24 Failure mode of specimen S2- FNV

Failure modes of horizontally loaded panels were different from horizontally loaded prisms. Figures 4.25, Figure 4.26 and Figure 4.27 show the failure mode of the hollow, partially grouted and fully grouted panels, respectively. The diagonal cracking which was pronounced in the case of prisms was not evident in the case of panels. The diagonal cracking was attributed to the confinement effect of the loading table, forcing the prisms to fail in shear. The lack of diagonal cracking indicates that the confinement effect was not significant in this case. The failure of panels was characterized by vertical cracking through mortar joints on the face-shell and vertical cracking through the web.

Figure 4.25 Failure mode of specimen S2- HNH

Figure 4.26 Failure mode of specimen S2- PNH

Figure 4.27 Failure mode of specimen S2- FNH

4.3.2.2 Grouting

Table 4.10 provides the mean compressive strength of prisms and panels used for determining the effect of grouting.

Table 4.10 Mean compressive strength of prisms and panels for grouting comparison

Specimen ID	Loading Orientation	Grouting	Mortar Strength (MPa)	Ultimate Load (N)	Mean Compressive Strength (MPa)	COV (%)
S1–H4NV	Vertical	Hollow	3.8	32,112	7.8 (3)	11.2
S1–P4NV	Vertical	Partially	3.8	40,762	6.9 (3)	15.0
S1–F4NV	Vertical	Fully	5.8	51,261	6.6 (3)	4.8
S1–H3NV	Vertical	Hollow	3.8	34,138	8.3 (2)	–
S1–F3NV	Vertical	Fully	5.6	53,192	6.9 (3)	9.8
S1–H5NV	Vertical	Hollow	3.8	38,150	9.3 (2)	–
S1–F5NV	Vertical	Fully	5.6	60,837	7.8 (3)	12.7
S1–H4SV	Vertical	Hollow	6.5	40,014	9.7 (2)	–
S1–P4SV	Vertical	Partially	8.6	50,376	8.5 (2)	–
S1–F4SV	Vertical	Fully	8.6	59,939	7.7 (3)	14.3
S1–H4NH	Horizontal	Hollow	5.2	67,005	10.6 (3)	12.5
S1–P4NH	Horizontal	Partially	5.6	58,539	9.2 (2)	–
S1– F4NH	Horizontal	Fully	5.3	127,884	7.2 (3)	7.6
S1– H4SH	Horizontal	Hollow	8.6	74,232	11.7 (2)	–
S1– P4SH	Horizontal	Partially	8.6	74,110	11.7 (2)	–
S1– F4SH	Horizontal	Fully	8.6	143,540	8.1 (2)	–
S2–HNV	Vertical	Hollow	4.0	49,780	5.3 (3)	10.0
S2–PNV	Vertical	Partially	4.0	67,790	4.0 (3)	9.0
S2–FNV	Vertical	Fully	4.0	65,860	3.2 (3)	5.6
S2–HNH	Horizontal	Hollow	4.0	48,940	5.2 (2)	–
S2–PNH	Horizontal	Partially	4.0	59,114	3.5 (2)	–
S2–FNH	Horizontal	Fully	4.0	62,664	3.0 (2)	–

When all other parameters were kept the same, hollow prisms attained the highest compressive strength which is followed by partially grouted and fully grouted prisms showed the lowest strength. This trend is in line with findings reported by others (Drysdale and Hamid 1979; Wong

and Drysdale 1985). This strength variation is mainly due to the effective area used in the calculation.

For vertically loaded prisms, the net areas of hollow and partially grouted prisms are about 53% and 76% of the net area of the fully grouted prisms. Although the ultimate load was the highest for fully grouted prisms, the large area led to a lower strength than partially grouted and hollow prisms. It is also noted that the ultimate load of the fully grouted prism is lower than the sum of the ultimate loads of the hollow prism and the grout column, which is due to the incompatibility of the grout and block material. The effect of grouting masonry prisms loaded vertically is illustrated in Figure 4.28. The mean compressive strength of a hollow 4-block high Type N prism is 13.5% and 17.3% higher than similar partially grouted and fully grouted prisms, respectively. Similar observation was made for 4-block high prisms constructed with Type S mortar as well as 3-block high and 5-block high prisms.

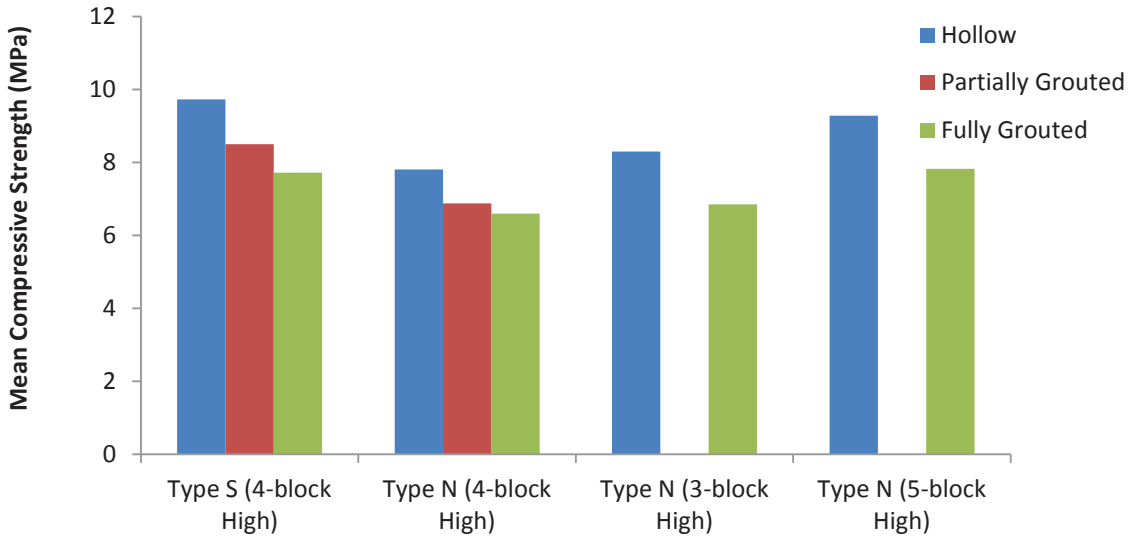

Figure 4.28 The effect of grouting on the compressive strength of prisms loaded normal to the bed joint

For horizontally loaded prisms, the net area of hollow and partially grouted prisms is 36% of that of fully grouted prisms. The effect of grouting masonry prisms loaded horizontally is illustrated in Figure 4.29. The horizontally loaded Type N hollow prisms showed 14.4% and 36.8% higher strength than partially grouted and fully grouted prisms, respectively. In the case of prisms with

Type S mortar, hollow and partially grouted prisms achieved similar strength and it was 44% higher than fully grouted prisms. In general, it can be concluded that for both loading directions, the effect of grouting situation on the compressive strength is consistent. As the grouting percentage increases, the compressive strength decreases.

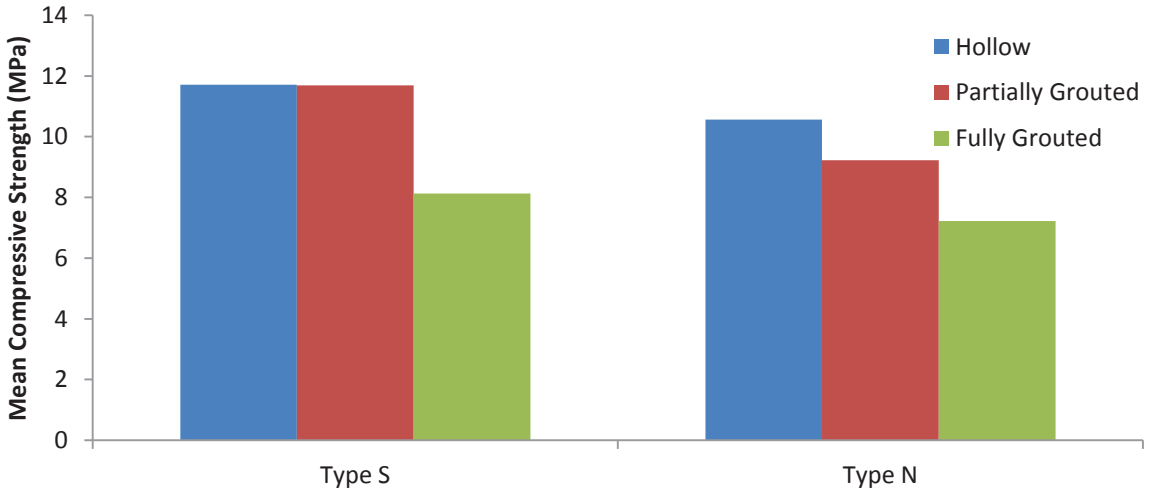

Figure 4.29 The effect of grouting on the compressive strength of prisms loaded parallel to the bed joint

Similar observations on the effect of grouting situation are made for panel specimens as shown in Figure 4.30. The average net area of hollow and partially grouted square panels is about 45% and 84% of that of fully grouted panels, respectively. Vertically loaded hollow specimens showed 33.1% and 67.3% higher compressive strengths than partially grouted and fully grouted panels, respectively.

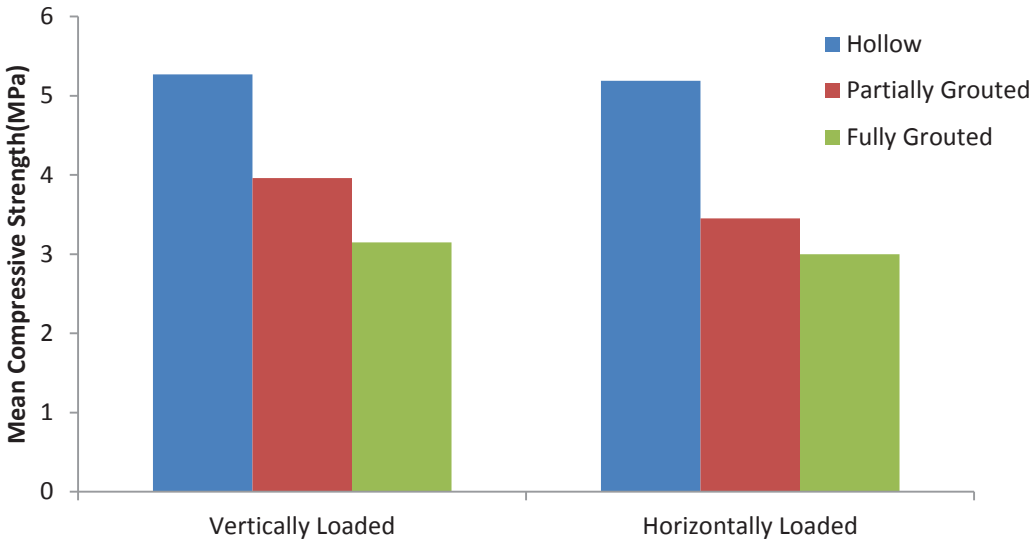

Figure 4.30 The effects of grouting horizontal and vertically loaded panels

Figure 4.31 correlates the percentage of grouting to the compressive strength for 4-high prisms and panel specimens vertically loaded. The strength on vertical axis is normalized by dividing the strength of fully grouted specimens. It shows that there seems to exist an approximately linear relationship between the percentage of grouting and the normalized strength although this relationship is different between the prisms and the panel specimens. The panel seems to produce higher normalized strength than the prisms.

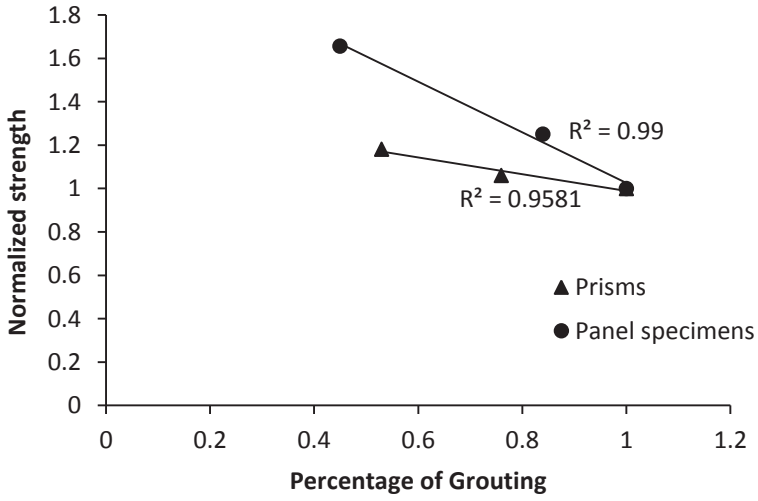

Figure 4.31 Normalized strength versus percentage of grouting for prisms and panels

4.3.2.3 Mortar Strength

Table 4.11 provides the mean compressive strength of prisms used for determining the effect of mortar strength.

Table 4.11 Mean compressive strength of prisms for mortar strength comparison

Specimen ID	Loading Orientation	Grouting	Mortar Strength (MPa)	Ultimate Load (N)	Mean Compressive Strength (MPa)	COV (%)
S1–H4NV	Vertical	Hollow	3.8	32,112	7.8 (3)	11.2
S1–H4SV	Vertical	Hollow	6.5	40,014	9.7 (2)	–
S1–P4NV	Vertical	Partially	3.8	40,762	6.9 (3)	15.0
S1–P4SV	Vertical	Partially	8.6	50,376	8.5 (2)	–
S1–F4NV	Vertical	Fully	5.8	51,261	6.6 (3)	4.8
S1–F4SV	Vertical	Fully	8.6	59,939	7.7 (3)	14.3
S1–H4NH	Horizontal	Hollow	5.2	67,005	10.6 (3)	12.5
S1– H4SH	Horizontal	Hollow	8.6	74,232	11.7 (2)	–
S1–P4NH	Horizontal	Partially	5.6	58,539	9.2 (2)	–
S1– P4SH	Horizontal	Partially	8.6	74,110	11.7 (2)	–
S1– F4NH	Horizontal	Fully	5.3	127,884	7.2 (3)	7.6
S1– F4SH	Horizontal	Fully	8.6	143,540	8.1 (2)	–

In general, prisms with Type S mortar showed higher compressive strength than prisms with Type N mortar for both loading directions and for all grouting configurations. The effects of mortar strength on the compressive strength of 4-high prisms loaded normal to the bed joint is illustrated in Figure 4.32. For all grouting configurations, prisms with Type S mortar showed an average of 22.5% higher strength than those with Type N mortar. The effect is more pronounced for hollow and partially-grouted prisms where 25% and 23% higher strengths respectively than Type N prisms with similar grouting configurations were observed. Fully-grouted Type S prisms showed 16% higher strength than fully-grouted Type N prisms.

The effects of mortar strength on the compressive strength of prisms loaded parallel to the bed joint is illustrated in Figure 4.33. Figure 4.33 shows that the use of Type S mortar resulted in an average of 16.8% higher prism strength than Type N mortar. The effect is more distinct for

partially grouted prisms where Type S mortar resulted in 27% higher prism strength than Type N mortar whereas this increase was 11% and 5% for hollow and fully-grouted prisms. Considering that the strength difference in Type N and S mortar used in this study was not significant, it may be extrapolated that a more pronounced prism strength increase can be expected if mortar strength had a greater difference. The typical failure modes for Type S prisms were similar to Type N prisms for both loading directions and grouting arrangements.

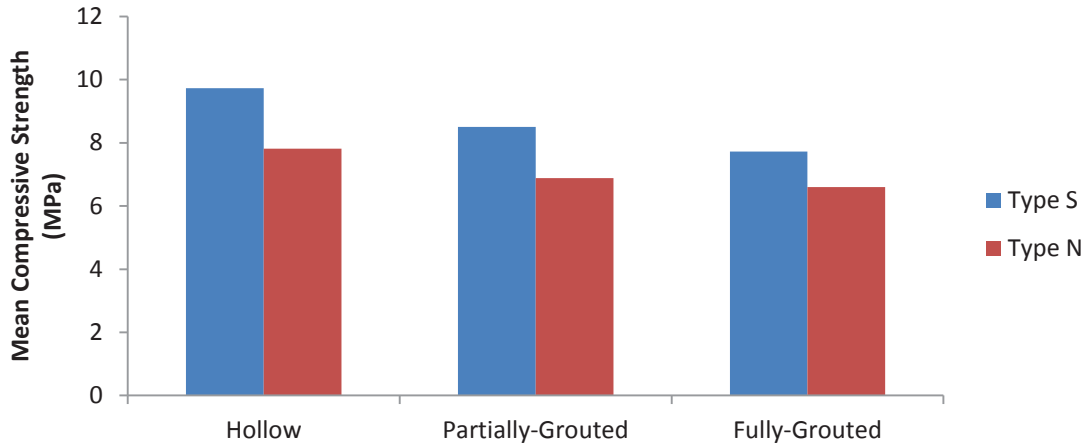

Figure 4.32 The effect of mortar strength on the compressive strength of 4-block high prisms loaded normal to the bed joint

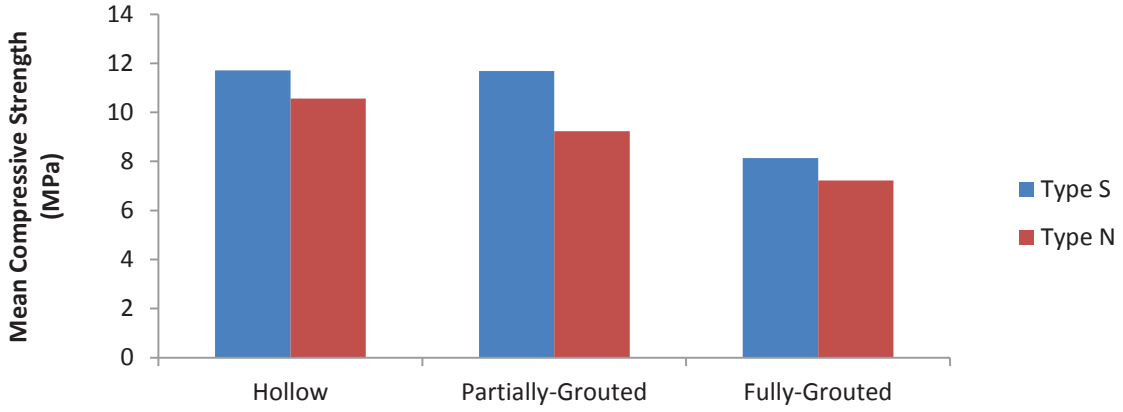

Figure 4.33 The effect of mortar strength on the compressive strength of 4-block high prisms loaded parallel to the bed joint

4.3.2.4 Central Web Interruption

Table 4.12 Mean compressive strength of prisms for central web interruption comparison

Specimen ID	Loading Orientation	Grouting	Mortar Strength (MPa)	Ultimate Load (N)	Mean Compressive Strength (MPa)	COV (%)
S1–F4SV	Vertical	Fully	8.6	59,939	7.7 (3)	14.3
S1–F4SVW	Vertical	Fully	6.7	50,013	6.4 (2)	–
S1– F4NH	Horizontal	Fully	5.3	127,884	7.2 (3)	7.6
S1-F4NHW	Horizontal	Fully	5.3	104,501	5.9 (3)	5.0
S1– F4SH	Horizontal	Fully	8.6	143,540	8.1 (2)	–
S1– F4SHW	Horizontal	Fully	6.7	67,306	3.8 (2)	–

Figure 4.34 shows the effect of central web on the prism strength for Type N and Type S prism loaded normal or parallel to the bed joint. The mean compressive strength for the prisms are found in Table 4.12. It can be seen that removing the central web has an effect on the overall compressive strength of prisms. For specimens S1-F4SV which was loaded vertically, the removal of central web resulted in an 18% reduction from the compressive strength of prisms with central web. This is attributed to the fact that the unit strength is higher than the mortar strength and replacing the web with a weaker material (mortar) caused the strength reduction.

In the case of horizontally loaded prisms, prisms with central web exhibited an average of 68% increase in strength when compared with prisms with central web removed. This is contrary to the current practice in the standard S304 where a less than unity reduction factor is suggested for prism strength if the web is present. The conventional thinking is that the presence of web interrupts the continuity of the grout therefore leads to a reduction of the strength. However, results herein showed that the central web contributes to the overall compressive strength of the prism more than the continuous grouted core since the strength of the grout is much lower than the compressive strength of the unit.

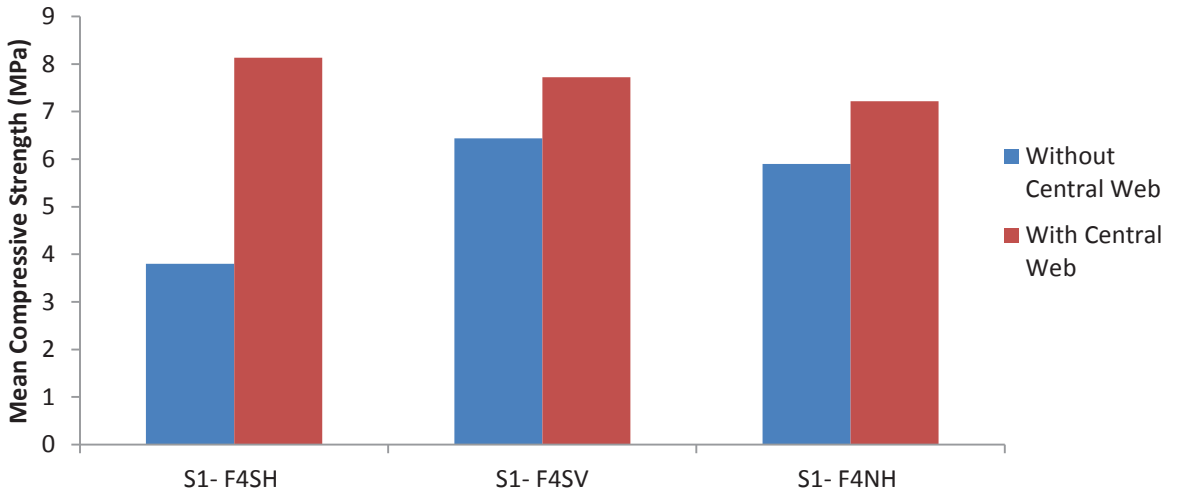

Figure 4.34 The effect of central web interaction on compressive strength of prisms

4.3.2.5 Height-to-thickness Ratio

Table 4.13 provides the mean compressive strength of prisms used for determining the effect of height-to-thickness ratio.

Table 4.13 Mean compressive strength of prisms for height-to-thickness ratio comparison

Specimen ID	Loading Orientation	Grouting	Mortar Strength (MPa)	Ultimate Load (N)	Mean Compressive Strength (MPa)	COV (%)
S1–H3NV	Vertical	Hollow	3.8	34,138	8.3 (2)	–
S1–H4NV	Vertical	Hollow	3.8	32,112	7.8 (3)	11.2
S1–H5NV	Vertical	Hollow	3.8	38,150	9.3 (2)	–
S1–F3NV	Vertical	Fully	5.6	53,192	6.9 (3)	9.8
S1–F4NV	Vertical	Fully	5.8	51,261	6.6 (3)	4.8
S1–F5NV	Vertical	Fully	5.6	60,837	7.8 (3)	12.7

The effect of height-to-thickness ratio on the compressive strength of prisms loaded normal to the bed joint is illustrated in Figure 4.35. It shows that the strength variation between the 3-block and 4-block high prisms was insignificant. The 5-block high prisms showed an average of 13% higher strength than the 3-block high prism. Prism height does not seem to have a pronounced effect on the compressive strength of prisms. This is different from some previous studies where an increase in the height-to-thickness ratio was shown to lead to a reduction in the prism compressive strength. This discrepancy is believed to attribute to the small size of the scaled block. The effect of the height was possibly outweighed by the inherent scatter in test results.

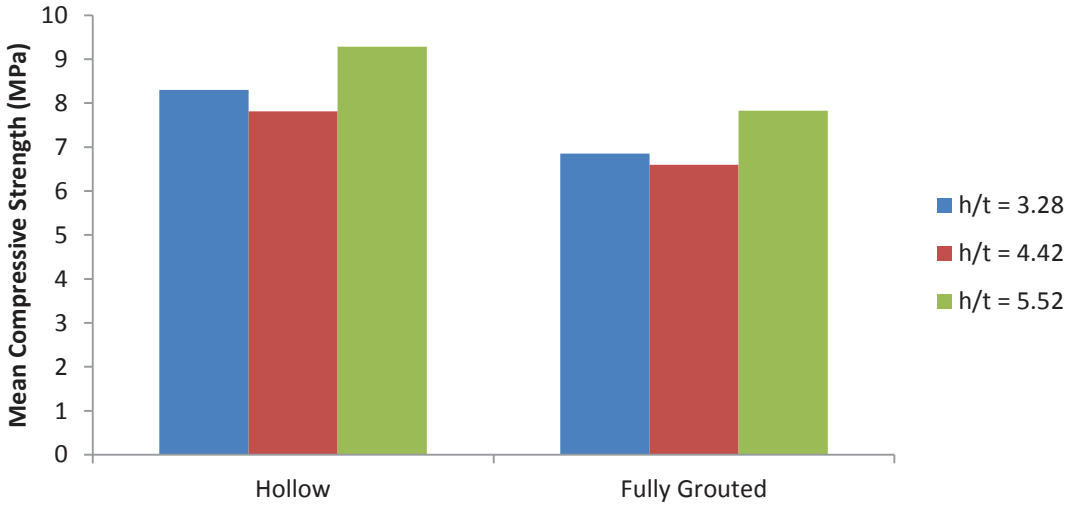

Figure 4.35 Effect of height-to-thickness ratio on the compressive strength of prisms loaded normal to the bed joint

Figure 4.36 and Figure 4.37 show the typical failure mode of 3-high (S1-H3NV) and 5- high (S1-F5NV) prisms, respectively. Failure of the 3-high prism was characterized by diagonal and vertical cracking, which led to face-shell spalling. The 5-high prism showed more vertical cracking through the face-shell and web.

Figure 4.36 Failure mode of specimen S1- H3NV

Figure 4.37 Failure mode of specimen S1- F5NV

4.4 SPECIMEN RESULTS– DIAGONALLY LOADED PANELS

In Series 2, twelve panels were loaded diagonally to obtain the masonry tensile strength. The results are summarized in Table 4.14. For diagonally loaded prisms, the net area of the specimen is calculated in accordance with equation [2.2] and then implemented in equation [2.1] to obtain the diagonal tensile stress.

Table 4.14 Compressive strength of panels loaded diagonally

Specimen ID	Grouting	Mortar Strength (MPa)	Net Area (mm^2)	Ultimate Load (N)	Diagonal Tensile Strength (MPa)
S2– HND	Hollow	5.5	13,797	7,220 (2)	0.37
S2– PND	Partially		22,500	19,413 (2)	0.61
S2– FND	Fully		26,754	30,652 (2)	0.81
S2– HSD	Hollow	6.5	13,797	7,362 (2)	0.38
S2– PSD	Partially		22,500	24,329 (2)	0.76
S2– FSD	Fully		26,754	37,568 (2)	0.99

For a given mortar type, the mean diagonal tensile strength increased as the panel grouting varied from hollow to partially grouted to fully grouted as shown in Figure 4.38. This is different from the prism compressive strength as affected by grouting discussed in previous sections. Failure of diagonally loaded panels involved a stepping crack pattern through the mortar joints running through the loaded corner as shown in Figure 4.39. Figure 4.40 shows the cross-section of the failure plane of these panels.

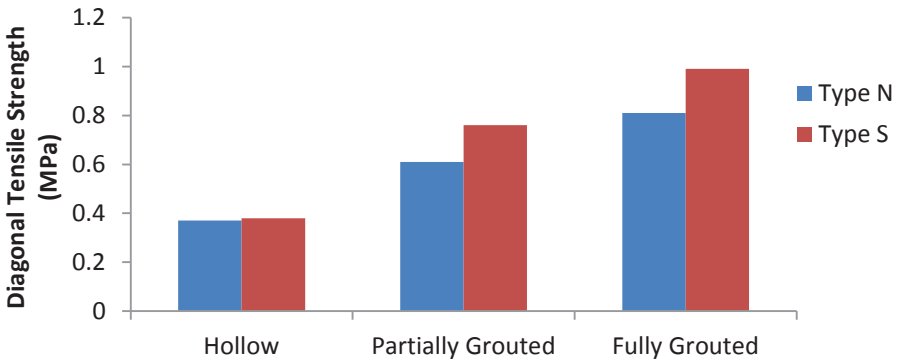

Figure 4.38 Effect of mortar strength on diagonally loaded panels

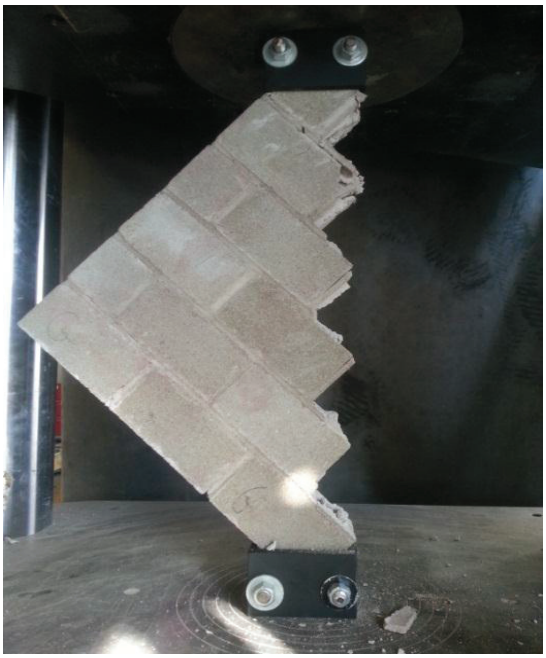

Figure 4.39 Typical failure mode of diagonally loaded panels

Hollow Partially Grouted Fully Grouted

Figure 4.40 Cross-section of failure plane of diagonally loaded panels

The increase in the tensile strength as a result of grouting is in line with findings reported in some previous studies (Drysdale et al. 1979; Maleki et al. 2007) where significant strength increases were observed when comparing fully grouted and hollow specimens. In this study, this strength increase was determined to be more than 200%. For a given grouting situation, the use of Type S mortar resulted in a higher tensile strength than Type N mortar, which is consistent with the findings obtained on prisms. The increase in tensile strength as a result of an increase in mortar strength was approximately 13%. The experimental diagonal tensile-to-compressive strength ratio for hollow, partially grouted and fully grouted type N specimens is 0.05, 0.09 and 0.12, respectively. Similarly, the experimental diagonal tensile-to-compressive strength ratio for hollow, partially grouted and fully grouted type S specimens is 0.04, 0.09 and 0.13, respectively. These values were in a similar order to those obtained by Mosalam (1996) and Drysdale and Hamid (1982). Mosalam (1996) reported a diagonal tensile-to-compressive strength ratio of 0.07 for hollow type S panels. Drysdale and Hamid (1982) found that the diagonal tensile-to-compressive strength ratio was 0.06 for hollow type S and type N panels.

CHAPTER 5 EVALUATION OF DESIGN METHODS

5.1 INTRODUCTION

In this chapter, the experimental results presented in Chapter 4 are used to evaluate the current code practice in two design considerations. First, the prism strengths are compared with the tabulated unit-mortar method provided by MSJC 2011 and the Canadian masonry design standard S304.1-04. Secondly, the results on the loading direction are used to evaluate the χ factor specified in the S304.1 in the context of infill strength comparison.

5.2 PRISM STRENGTH COMPARISONS

5.2.1 ASTM and CSA Correction Factors

The compressive strength of vertically loaded masonry prisms and panels are adjusted using the height-to-thickness correction factors provided by ASTM C1314 (2011) and CSA S304.1-04 (2004). This adjustment is not required for horizontally loaded prisms and panels. In ASTM C1314 (2011), the correction factors do not differentiate between grouting arrangements. ASTM provides correction factors up to an h/t ratio of 5; thus for the prisms with h/t ratio of 5.52 and panels with h/t ratio of 6.68 the correction factor for h/t ratio of 5 was used. For prisms with an h/t ratio of 3.28, 4.42 and 5.52, the ASTM correction factors are 1.094, 1.178 and 1.22 respectively regardless of the grouting arrangement. Annex D of CSA S304.1-04 provides a factor of 1.0 for all hollow and partially grouted prisms that is applied to all height-to-thickness ratios. For fully grouted prisms with h/t ratio of 3.28, 4.42 and 5.52, the CSA correction factors were determined to be 0.92, 0.97 and 1.0, respectively.

Table 5.1 lists the compressive strength of vertically loaded prisms and panels before and after multiplying the corresponding correction factors that have been provided by ASTM C1314 (2011) and CSA S304.1 -04 (2004).

Table 5.1 Compressive strength of vertically loaded specimens with correction factors

Specimen ID	h/t Ratio	Mean Compressive Strength (MPa)	ASTM Correction Factor	ASTM Modified Compressive Strength (MPa)	CSA Correction Factor	CSA Modified Compressive Strength (MPa)
S1–H3NV	3.28	8.3	1.094	9.1	1.00	8.3
S1–F3NV	3.28	6.9	1.094	7.5	0.92	6.3
S1–H4NV	4.42	7.8	1.178	9.2	1.00	7.8
S1–P4NV	4.42	6.9	1.178	8.1	1.00	6.9
S1–F4NV	4.42	6.6	1.178	7.8	0.97	6.4
S1–H5NV	5.52	9.3	1.220	11.3	1.00	9.3
S1–F5NV	5.52	7.8	1.220	9.6	1.00	7.8
S1–H4SV	4.42	9.7	1.178	11.5	1.00	9.7
S1–P4SV	4.42	8.5	1.178	10.0	1.00	8.5
S1–F4SV	4.42	7.7	1.178	9.1	0.97	7.5
S1–F4SVW	4.42	6.4	1.178	7.6	0.97	6.2
S2–HNV	6.68	5.3	1.220	6.4	1.00	5.3
S2–PNV	6.68	4.0	1.220	4.8	1.00	4.0
S2–FNV	6.68	3.2	1.220	3.8	1.00	3.2

Figure 5.1 and Figure 5.2 illustrate the effect of height-to-thickness correction factors on the average compressive strength for vertically loaded prisms and panels for ASTM and S304.1 standards, respectively. It is noted that the modified f'_m values using ASTM correction factors are all greater than the experimentally obtained strength whereas those using S304 correction factors are either unchanged from or slightly lower than the test results.

Two different philosophies were used in the development of ASTM and S304.1 correction factors. While the ASTM considers an h/t ratio of 2 as the standard height-to-thickness ratio and corrects for other ratios with factors greater than unity, the Canadian S304.1 considers an h/t ratio of 5 as the standard and applies a reduction factor for smaller h/t ratios with exception of hollow and partially grouted prisms. For the latter two cases, the S304.1 correction factor is one, indicating that height-to-thickness ratio has no effect. The test results did not show a reduction trend with an increase in the height-to-thickness ratio regardless of hollow or grouted prisms (discussed in Chapter 4). The maximum variation of the ultimate strength within the three height-to-thickness ratios (about 13%) is considered relatively small. The results seem to suggest

that S304.1-04 correction factor for hollow prisms is reasonable but put the S304.1 practice of using a reduction factor for fully grouted prisms in question.

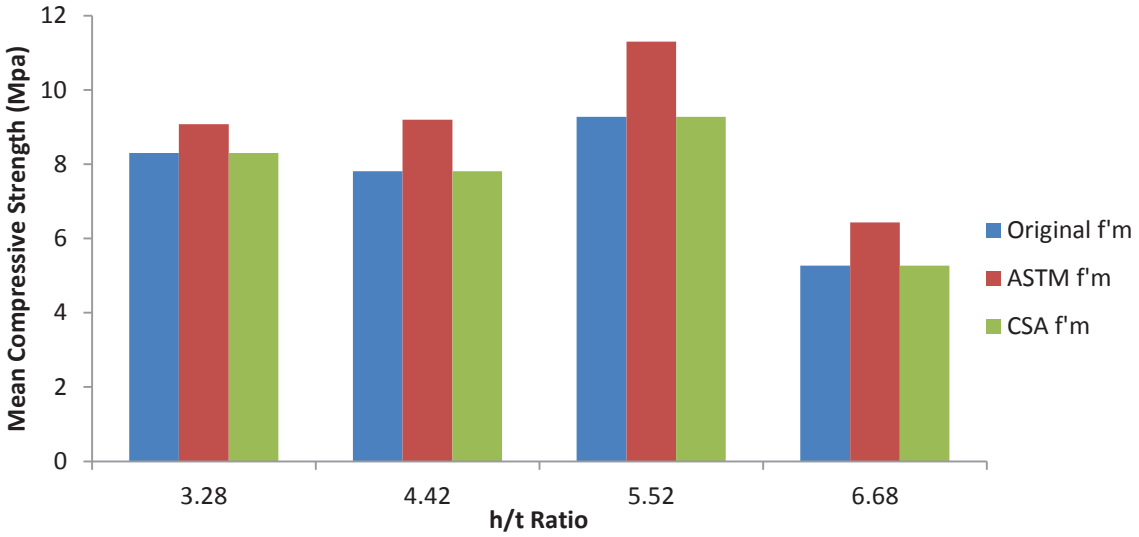

Figure 5.1 Effect of height-to-thickness correction factors on compressive strength of hollow prisms and panels – Type N mortar

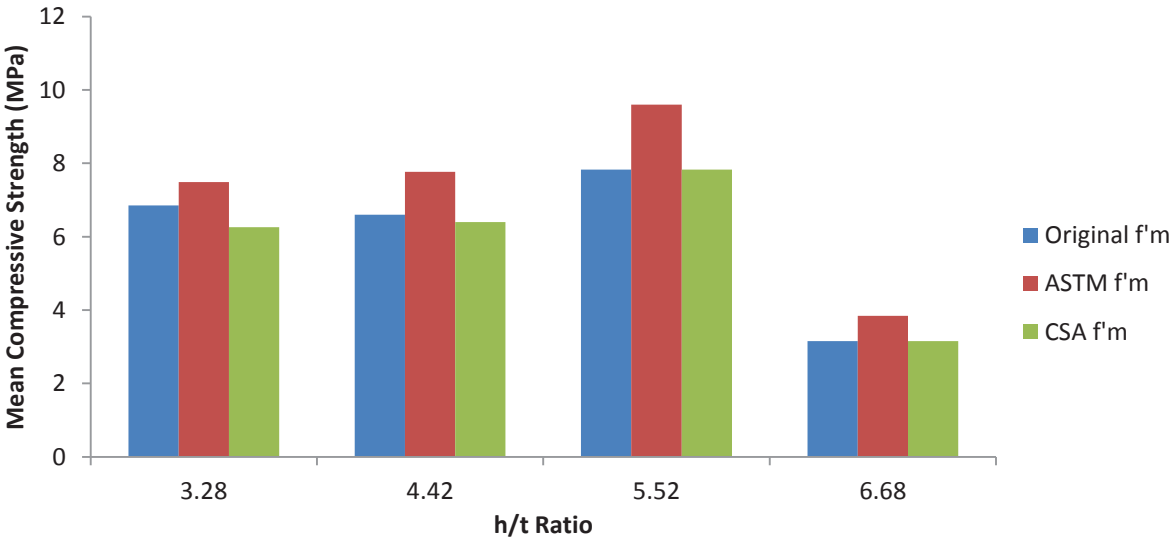

Figure 5.2 Effect of height-to-thickness correction factors on compressive strength of fully-grouted prisms and panels – Type N mortar

5.2.2 Comparison of Test Results with Unit-Mortar Method

This section deals with the strength comparison of experimental results and values obtained from the current design standards. As an alternative to prism testing for determination of f'_m values, both the MSJC 2011 and Canadian S304.1-04 specify a unit-mortar method where the f'_m values are determined based on the unit strength and type of mortar. This method is usually presented in a tabulated manner and interpolation between values is permitted. This method is calibrated based on prism testing results obtained decades ago and a re-evaluation is needed. In this study, two unit strengths were involved in construction of specimens. The average compressive strengths of frog-end and flat-end units are 19.3MPa and 14.1MPa, respectively. Prisms were only composed of frog-end units, whereas the panels are composed of both block units. For panels, the average compressive strength of the unit was taken to be 16.7MPa.

Table 5.2 provides a comparison between the experimental f'_m values with correction factor applied and those obtained by unit-mortar method. As can be seen, the tabulated values in both the American and Canadian standards over-estimate the compressive strength. For example, MSJC overestimates the strength for Type N prisms, Type S prisms and Type N panels by 18%, 18% and 49% respectively. The corresponding overestimations by CSA S304.1 for Type N prisms, Type S prisms and Type N panels are 11%, 27% and 46%. The performance of both standards is comparable for prisms while the CSA S304.1 had a better correlation with results with COV values lower than those by MSJC. In the case of panels, an average strength of frog-end and flat-end units is used. If the flat-end strength (lower of the two = 14.1 MPa) is used, the tabulated CSA value for f'_m for hollow, partially grouted and fully grouted panels are 7.6, 6.7 and 5.7 (Table 4, CSA S304.1-04); whereas the tabulated MSJC value is 8.4 (Table 2, MSJC 2011). The average experimental-to-tabulated ratios for panels are then determined to be 0.60 and 0.62 for MSJC and S304.1 respectively. Although they provide improvement, the overestimation by both standards is still significant. It suggests that panels should not be used in the f'_m determination. Although they represent the actual construction configuration, the results may give superficially low strength values. Secondly, if different unit strength is used in the construction, the f'_m value based on unit-mortar method should be based on the weakest unit strength.

Table 5.2 Comparison of experimental f'$_m$ to tabulated values

Specimen ID	Modified f'$_m$ (MSJC, CSA) (MPa)	MSJC Tabulated (MPa)	Experimental / MSJC Tabulated	CSA Tabulated (MPa)	Experimental/ CSA Tabulated
S1–H3NV	(9.1,8.3)	10.9	0.83	9.7	0.86
S1–F3NV	(7.5, 6.3)	10.9	0.69	7.3	0.86
S1–H4NV	(9.2,7.8)	10.9	0.84	9.7	0.80
S1–P4NV	(8.1, 6.9)	10.9	0.74	9.0	0.77
S1–F4NV	(7.8, 6.4)	10.9	0.72	7.3	0.88
S1–H5NV	(11.3, 9.3)	10.9	1.04	9.7	0.96
S1–F5NV	(9.6, 7.8)	10.9	0.88	7.3	1.07
		Avg.	0.82		0.89
		COV (%)	14.6		11.4
S1–H4SV	(11.5,9.7)	11.7	0.98	12.6	0.77
S1–P4SV	(10,8.5)	11.7	0.85	11.7	0.73
S1–F4SV	(9.1,7.5)	11.7	0.78	9.7	0.77
S1–F4SVW	(7.6, 6.2)	11.7	0.65	9.7	0.64
		Avg.	0.82		0.73
		COV (%)	17.0		8.4
S2–HNV	(6.4, 5.3)	9.7	0.66	8.7	0.61
S2–PNV	(4.8, 4.0)	9.7	0.49	7.7	0.52
S2–FNV	(3.8, 3.2)	9.7	0.39	6.5	0.49
		Avg.	0.51		0.54
		COV (%)	26.6		11.6

Figure 5.3 and Figure 5.4 compare the modified compressive strength with the unit-mortar method from mortar point of view based on CSA S304.1 and MSJC, respectively. They show that since the MSJC unit-mortar method does not consider grouting situation, for a given mortar type (N), it has one constant value. This value compares well with hollow prism results but overestimates the strength for grouted prisms for varying mortar strength. On the other hand, the CSA S304.1 unit-mortar method provides strength values for different grouting situation. As seen in Figure 5.3, the S304.1 method, in general, provides more representative values with experimental data. It also shows that as the mortar strength increases, the correlation between the method values and the test results become better.

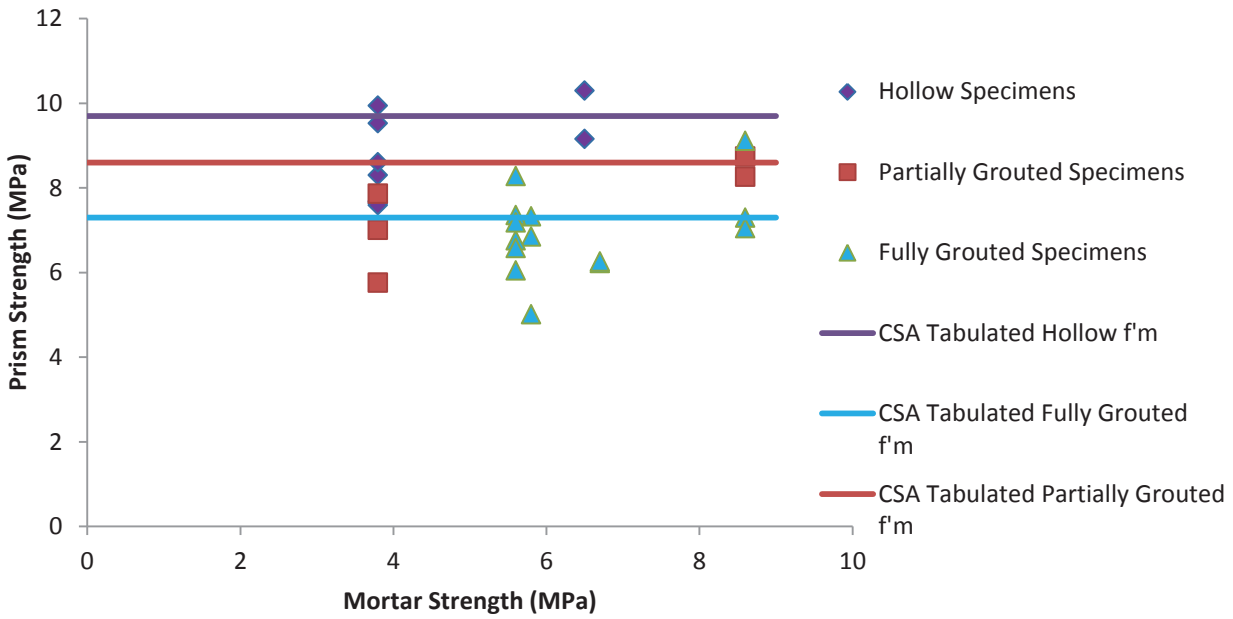

Figure 5.3 CSA modified prism compressive strength vs. mortar strength

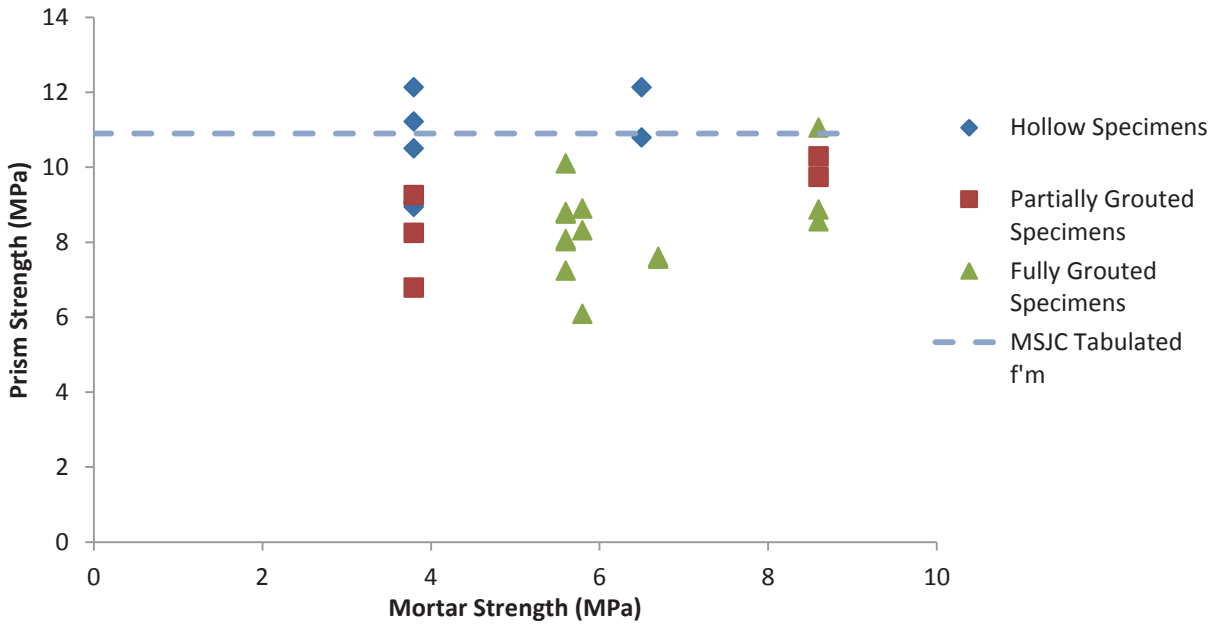

Figure 5.4 MSJC modified prism compressive strength vs. mortar strength

The comparison studies of the unit-mortar method performed by other researchers using their test results have produced inconsistent findings. While majority of them found that CSA S304.1

method tends to under-estimate the prism strength (Hamid et al. 1985; Wong and Drysdale 1985; Hedstorm and Hogan 1990; Steadman et al. 1995), some reported overestimation by the method (Soon 2011; Menash and Liu 2013). It is noted that however, the former finding was often obtained from prisms constructed with medium to strong unit with relatively strong mortar. When a medium strength unit combined with a relatively weak mortar was used as in the case of this study, the unit-mortar strength method tends to overestimate the strength. More data points are required to cover more combinations of unit and mortar strength in the test to make definitive conclusions.

5.3 INFILL STRENGTH COMPARISONS

This section summarizes the test results of in-plane strength of masonry infills from the available literature which are used in the comparison analysis with design methods in CSA S304 and MSJC 2011.

5.3.1 Previous Experimental Programs in the Literature

Although more test results are reported in the literature, only those with all key material properties provided are used in the consideration. These specimens listed below were all considered as standard with no openings in the infill and no gaps between the infill and the bounding frame.

Yong [YN] (1983), McBride [MC] (1984), Amos [AM] (1985) and Richardson [RC] (1986) all conducted research on concrete masonry infilled steel frames under a racking load applied at the top beam. The frame was composed of W200x46 for the columns and W250x58 for the beam. The columns were oriented for bending around the weak axis, while the beam was oriented for bending along its strong axis. The infill material was composed of standard 200 mm hollow concrete blocks and panel dimensions were 3.6 m long by 2.8 m high.

Riddington [RD] (1984) performed full scale tests on concrete block masonry infilled steel frames. Both flexible and stiff steel frames were examined with an infill wall constructed of 440 x 215 x 100 mm blocks.

Flanagan [FL] (1994) tested structural clay tile infilled steel frames under in-plane load. Both single wythe panels were constructed of nominally 8 inch (203 mm) thick tile units and double wythe panels were constructed of nominally 8 inch and 4 inch (102 mm) tile units creating a 13 inch wall (330 mm). Panels were constructed in running bond using Type N masonry cement.

Mehrabi et al. [MH] (1996) conducted tests on masonry infilled reinforced concrete frames under lateral load. Infill was constructed using hollow and solid concrete masonry blocks.

Soon [SN] (2011) tested 9 masonry infilled steel frames. The infill material was composed of one-third scale 200 mm concrete masonry blocks with type S mortar. The column and beam was made up of W100 x 19. All specimens were either partially grouted or fully grouted.

Tables 5.3 and 5.4 provide descriptions of test setup, geometric and material properties of both the infill and frame for above mentioned studies. This information is needed in the calculation of design strength using standards.

Table 5.3 Frame properties of experimental studies

Author	ID	Material	E (MPa)	Beam		Column	
				Size (mm x mm)	I(x 10^7 mm^4)	Size (mm x mm)	I (x 10^7 mm^4)
YN(1983)	1A	Steel	200,000	W200x46	4.54	W250x58	1.88
YN(1983)	2B	Steel	200,000	W200x46	4.54	W250x58	1.88
YN(1983)	3B	Steel	200,000	W200x46	4.54	W250x58	1.88
YN(1983)	6E	Steel	200,000	W200x46	4.54	W250x58	1.88
RD(1984)	2a	Steel	200,000	152x152x30 UC	1.75	152x152x30 UC	1.75
RD(1984)	2b	Steel	200,000	406x140x39 UB	12.5	406x140x39 UB	12.5
MC(1984)	WA1	Steel	200,000	W200x46	4.54	W250x58	1.88
MC(1984)	WA2	Steel	200,000	W200x46	4.54	W250x58	1.88
MC(1984)	WA3	Steel	200,000	W200x46	4.54	W250x58	1.88
MC(1984)	WA4	Steel	200,000	W200x46	4.54	W250x58	1.88
MC(1984)	WA5	Steel	200,000	W200x46	4.54	W250x58	1.88

UC – British Universal Columns

UB – British Universal Beams

Table 5.3 (continued) Frame properties of experimental studies

Author	ID	Material	E (MPa)	Beam		Column	
				Size (mm x mm)	I (x 10^7 mm^4)	Size (mm x mm)	I (x 10^7 mm^4)
AM(1985)	WC1	Steel	200,000	W200x46	4.54	W250x58	1.88
AM(1985)	WC2	Steel	200,000	W200x46	4.54	W250x58	1.88
AM(1985)	WC3	Steel	200,000	W200x46	4.54	W250x58	1.88
AM(1985)	WC4	Steel	200,000	W200x46	4.54	W250x58	1.88
AM(1985)	WC5	Steel	200,000	W200x46	4.54	W250x58	1.88
AM(1985)	WC6	Steel	200,000	W200x46	4.54	W250x58	1.88
AM(1985)	WC7	Steel	200,000	W200x46	4.54	W250x58	1.88
AM(1985)	WC8	Steel	200,000	W200x46	4.54	W250x58	1.88
RC(1986)	WD5	Steel	208,000	W200x46	4.54	W250x58	1.88
RC(1986)	WD6	Steel	208,000	W200x46	4.54	W250x58	1.88
RC(1986)	WD7	Steel	208,000	W200x46	4.54	W250x58	1.88
RC(1986)	WD8	Steel	208,000	W200x46	4.54	W250x58	1.88
RC(1986)	WD9	Steel	208,000	W200x46	4.54	W250x58	1.88
RC(1986)	WD10	Steel	208,000	W200x46	4.54	W250x58	1.88
RC(1986)	WD12	Steel	208,000	W200x46	4.54	W250x58	1.88
FL(1994)	1	Steel	200,000	W310x52	11.9	W250x18	0.091
FL(1994)	2	Steel	200,000	W310x52	11.9	W250x45	0.703
FL(1994)	3	Steel	200,000	W310x52	11.9	W250x67	2.22
FL(1994)	4	Steel	200,000	W460x113	55.6	W410x39	0.404
FL(1994)	5	Steel	200,000	W460x67	29.5	W410x60	1.20
FL(1994)	9	Steel	200,000	W310x52	11.9	W250x45	7.11
FL(1994)	17	Steel	200,000	W310x52	11.9	W250x45	0.703
FL(1994)	21a	Steel	200,000	W310x52	11.9	W250x45	0.703
MH(1996)	SP3	RC	21,925	152x229	15.2	178x178	8.37
MH(1996)	SP4	RC	17,237	152x229	15.2	178x178	8.37
MH(1996)	SP8	RC	17,237	152x229	15.2	178x178	8.37
MH(1996)	SP9	RC	17,237	152x229	15.2	178x178	8.37
MH(1996)	SP10	RC	17,237	152x229	15.2	178x178	8.37
SN(2011)	P1NA	Steel	200,000	W100x19	0.477	W100x19	0.477
SN(2011)	F1NA	Steel	200,000	W100x19	0.477	W100x19	0.477
SN(2011)	P3NA	Steel	200,000	W100x19	0.477	W100x19	0.477
SN(2011)	P3NA	Steel	200,000	W100x19	0.477	W100x19	0.477
SN(2011)	P3NI	Steel	200,000	W100x19	0.477	W100x19	0.161
SN(2011)	F3NI	Steel	200,000	W100x19	0.477	W100x19	0.161

RC – Reinforced concrete

Table 5.4 Infill properties of experimental studies

Author	ID	Grout	Material	f'_m (MPa)	E_I (MPa)	h (mm)	l (mm)	t (mm)
YN(1983)	1A	Hollow	CMU	23.7	20,000*	2,800	3,600	200
YN(1983)	2B	Hollow	CMU	33.3	20,000*	2,800	3,600	200
YN(1983)	3B	Hollow	CMU	31.4	20,000*	2,800	3,600	200
YN(1983)	6E	Hollow	CMU	35.4	20,000*	2,800	3,600	200
RD(1984)	2a	Solid	Block	7.0	15,400	2710	2710	100
RD(1984)	2b	Solid	Block	7.0	15,400	2485	2485	100
MC(1984)	WA1	Hollow	CMU	27.4	14,200	2,800	3,600	200
MC(1984)	WA2	Hollow	CMU	27.7	14,200	2,800	3,600	200
MC(1984)	WA3	Hollow	CMU	26.5	14,200	2,800	3,600	200
MC(1984)	WA4	Hollow	CMU	24.4	14,200	2,800	3,600	200
MC(1984)	WA5	Hollow	CMU	25.6	14,200	2,800	3,600	200
AM(1985)	WC1	Hollow	CMU	31.7	20,000*	2,800	3,600	200
AM(1985)	WC2	Hollow	CMU	27.7	11,400	2,800	3,600	200
AM(1985)	WC3	Hollow	CMU	30.9	20,000*	2,800	3,600	200
AM(1985)	WC4	Hollow	CMU	33.1	21,650	2,800	3,600	200
AM(1985)	WC5	Hollow	CMU	32.5	20,000*	2,800	3,600	200
AM(1985)	WC6	Hollow	CMU	30.9	20,000*	2,800	3,600	200
AM(1985)	WC7	Hollow	CMU	33.4	17,500	2,800	3,600	200
AM(1985)	WC8	Hollow	CMU	33.3	19,000	2,800	3,600	200
RC(1986)	WD5	Hollow	CMU	29.4	19,000	2,800	3,600	200
RC(1986)	WD6	Hollow	CMU	26.3	17,300	2,800	3,600	200
RC(1986)	WD7	Hollow	CMU	25.4	18,000	2,800	3,600	200
RC(1986)	WD8	Hollow	CMU	28.1	17,700	2,800	3,600	200
RC(1986)	WD9	Hollow	CMU	24.6	19,800	2,800	3,600	200
RC(1986)	WD10	Hollow	CMU	25.3	17,000	2,800	3,600	200
RC(1986)	WD12	Hollow	CMU	24.2	15,500	2,800	3,600	200
FL(1994)	1	Hollow	SCT	5.6	5,295	2,235	2,235	195
FL(1994)	2	Hollow	SCT	5.6	5,295	2,235	2,235	195
FL(1994)	3	Hollow	SCT	5.6	5,295	2,235	2,235	195
FL(1994)	4	Hollow	SCT	2.3	5,040	2,235	2,235	330
FL(1994)	5	Hollow	SCT	2.3	5,040	2,235	2,235	330
FL(1994)	9	Hollow	SCT	5.6	5,295	2,235	2,235	195
FL(1994)	17	Hollow	SCT	5.6	5,295	2,235	3,454	195
FL(1994)	21a	Hollow	SCT	5.6	5,295	2,235	2,845	195

* - Value not provided in literatures, E_I value of $850f'_m$ was assumed, but not greater than 20,000 MPa
CMU- Concrete Masonry Unit
SCT- Structural Clay Tile

Table 5.4 (continued) Infill properties of experimental studies

Author	ID	Grout	Material	f'_m (MPa)	E_I (MPa)	h (mm)	l (mm)	t (mm)
MH(1996)	SP3	Solid	CMU	15.1	9,522	1,422	2,032	100
MH(1996)	SP4	Hollow	CMU	10.6	4,596	1,422	2,032	100
MH(1996)	SP8	Hollow	CMU	9.5	5,102	1,422	2,032	100
MH(1996)	SP9	Solid	CMU	14.2	8,239	1,422	2,032	100
MH(1996)	SP10	Hollow	CMU	10.6	8,840*	1,422	2,946	100
SN(2011)	P1NA	Partial	CMU	8.6	10,496	1,080	1,080	64
SN(2011)	F1NA	Fully	CMU	9.9	14,430	1,080	1,080	64
SN(2011)	P3NA	Partial	CMU	8.0	10,496	1,080	1,351	64
SN(2011)	F3NA	Fully	CMU	11.3	14,430	1,080	1,351	64
SN(2011)	P6NA	Partial	CMU	11.3	10,496	1,080	1,758	64
SN(2011)	P3NI	Partial	CMU	11.3	10,496	1,080	1,351	64
SN(2011)	F3NI	Fully	CMU	8.0	14,430	1,080	1,351	64

* - Value not provided in literatures, E_I value of $850f'_m$ was assumed. but not greater than 20,000 MPa
CMU- Concrete Masonry Unit

5.3.2 Comparison of Test Results from Literature with Design Methods

According to CSA S304.1 and MSJC 2011, the design ultimate strength is calculated using equations [2.6] and [2.9], respectively. The strength calculated using the design methods in CSA S304.1 and MSJC is intended for the infill strength only. Since the infill frame members in the test was essentially rigidly connected and as such, the lateral load is shared between the frame and the infill with the latter taking a large portion. In order for the design strength to be compared with the experimental load from literature, a coefficient needs to be applied to the design strength. The coefficient was obtained as follows. A linear analysis was conducted using computer software S-Frame. The properties of the frame and strut were input in the model and a 1kN horizontal force was applied at the roof level. The force resulted in the diagonal strut was then obtained. The value of the horizontal component of this diagonal force is the share taken by the infill and therefore it is the coefficient. The design strengths presented in the following sections are those obtained using analytical equations divided by the coefficient as appropriate.

Table 5.5 shows the comparison of the design ultimate strength with the experimental result of each specimen. It can be seen that results from different sources are quite scattered. For most

groups of results (except for one), MSJC underestimates the infill strength and this underestimation varies between 8 to 54% with a mean of 28%. Since the MSJC uses a constant diagonal strut width of 150 mm for all infills, the marked disparity with test results indicates that this method is questionable. On the other hand, the CSA S304.1 underestimates the ultimate strength by an overall average of 22%. However, the ultimate strength of specimens associated with Amos (1985), and Richardson (1986) was over-estimated by over 30%. It is noted that in those two cases, the reported infill material strength f'_m was unusually high while f'_m values for other groups were more representative of the real construction. It seems to suggest that for very strong masonry infills, the CSA S304.1 over-estimates the infill strength. For masonry infills of typical material strength (≤ 20 MPa), the CSA S304.1 provides conservative values for infill strength. It should also be pointed out that for concrete infilled frames; both MSJC and S304.1 are conservative, underestimating infill strength by about 40%.

Table 5.5 Ultimate strength comparison with results from available literature

Author	ID	P_{EXP} (kN)	CSA			
			P_{CSA} (χ=0.5) (kN)	P_{CSA}/P_{EXP}	P_{MSJC} (kN)	P_{MSJC}/P_{EXP}
YN(1983)	1A	448.8	396.6	0.80	290.2	0.64
YN(1983)	2B	538.2	508.7	0.86	366.4	0.67
YN(1983)	3B	556.8	487.3	0.79	346.3	0.61
YN(1983)	6E	422.6	532.0	1.14	387.9	0.90
			Avg.	0.90		0.71
			COV (%)	18.7		19.1
RD(1984)	2a	210.0	96.1	0.46	116.9	0.56
RD(1984)	2b	410.0	146.6	0.36	146.8	0.36
			Avg.	0.41		0.46
MC(1984)	WA1	471.0	441.8	0.94	316.1	0.67
MC(1984)	WA2	440.0	443.6	1.01	319.5	0.73
MC(1984)	WA3	463.0	427.2	0.92	305.6	0.66
MC(1984)	WA4	476.0	397.7	0.84	281.4	0.59
MC(1984)	WA5	445.0	414.6	0.93	295.3	0.66
			Avg.	0.93		0.66
			COV (%)	6.6		7.5

Table 5.5 (continued) Ultimate strength comparison with results from available literature

Author	ID	P_{EXP} (kN)	CSA			
			P_{CSA} (χ=0.5) (kN)	P_{CSA}/P_{EXP}	P_{MSJC} (kN)	P_{MSJC}/P_{EXP}
AM(1985)	WC1	420.0	454.3	1.08	349.7	0.82
AM(1985)	WC2	310.0	460.5	1.49	326.2	1.03
AM(1985)	WC3	285.0	446.3	1.57	341.2	1.17
AM(1985)	WC4	335.0	490.2	1.46	369.9	1.08
AM(1985)	WC5	245.0	462.8	1.89	357.7	1.43
AM(1985)	WC6	365.0	446.3	1.22	341.2	0.92
AM(1985)	WC7	534.0	510.9	0.96	378.8	0.69
AM(1985)	WC8	445.0	504.3	1.13	375.4	0.83
			Avg.	1.35		1.00
			COV	22.7		23.6
RC(1986)	WD5	334.0	448.9	1.34	301.4	0.90
RC(1986)	WD6	623.0	401.7	0.64	271.4	0.44
RC(1986)	WD7	494.0	388.9	0.79	261.5	0.53
RC(1986)	WD8	200.0	432.1	2.16	289.6	1.45
RC(1986)	WD9	267.0	381.3	1.43	251.3	0.94
RC(1986)	WD10	278.0	393.0	1.41	261.5	0.94
RC(1986)	WD12	196.0	385.4	1.97	249.5	1.27
			Avg.	1.39		0.92
			COV (%)	39.9		39.3
FL(1994)	1	164.0	38.2	0.23	28.6	0.19
FL(1994)	2	173.0	41.9	0.24	28.6	0.24
FL(1994)	3	153.0	49.8	0.33	28.6	0.36
FL(1994)	4	213.0	31.3	0.15	23.4	0.13
FL(1994)	5	172.0	33.0	0.19	23.4	0.19
FL(1994)	9	179.0	67.1	0.37	28.6	0.41
FL(1994)	17	193.0	60.9	0.32	28.6	0.21
FL(1994)	21a	181.0	51.3	0.28	28..6	0.22
			Avg.	0.26		0.49
			COV (%)	28.4		28.1

Table 5.5 (continued) Ultimate strength comparison with results from available literature

Author	ID	P_{EXP} (kN)	CSA			
			P_{CSA} (χ=0.5) (kN)	P_{CSA}/P_{EXP}	P_{MSJC} (kN)	P_{MSJC}/P_{EXP}
MH(1996)	SP3	277.7	203.5	0.73	300.0	1.08
MH(1996)	SP4	251.5	67.7	0.27	104.7	0.42
MH(1996)	SP8	190.0	62.3	0.33	90.4	0.48
MH(1996)	SP9	292.8	182.5	0.62	275.7	0.94
MH(1996)	SP10	293.5	84.9	0.29	85.0	0.29
			Avg.	0.42		0.59
			COV	49.7		56.4
SN(2011)	P1NA	111.0	41.0	0.37	87.0	0.78
SN(2011)	F1NA	156.9	59.5	0.38	128.6	0.82
SN(2011)	P3NA	93.8	45.5	0.49	79.5	0.85
SN(2011)	F3NA	131.7	77.5	0.59	144.4	1.1
SN(2011)	P6NA	104.2	72.4	0.69	111.9	1.07
SN(2011)	P3NI	78.9	56.5	0.72	76.2	0.97
SN(2011)	F3NI	121.9	67.8	0.56	79.3	0.65
			Avg.	0.54		0.89
			COV (%)	25.5		18.3
			Overall Avg.	0.78		0.72
			COV (%)	56.2		28.4

5.3.3 Comparison of Test Results with Design Methods with different χ factors

As discussed earlier, CSA S301.1 underestimates the design strength by an overall average of 22% when the χ factor was taken to be 0.5. In the experimental program, the prism and panel horizontal-to-vertical strength was found to be 1.5 for prisms and 0.94 for panels. Due to the confinement effect, panel results are believed to be more reasonable. To evaluate the effect of χ factor in the infill strength calculation, the CSA S304.1 values are re-calculated using χ factor of 0.94 and 0.7, an approximately average of 0.5 and 0.94. Table 5.6 shows the comparison of the design ultimate strengths calculated with χ= 0.7 and γ= 0.94 with the experimental results of each specimen. As shown in the table, the overall average design-to-experimental strength ratio using a χ factor of 0.94 was found to be 1.32 with an overall COV value of 50.8%. This shows that a χ factor of 0.94 is not acceptable to be used in the infill strength. A χ factor of 0.7 was then

considered in which the overall average design-to-experimental strength ratio 1.03 with an overall COV value of 50.5%. The $\chi = 0.7$ improved the strength estimate.

Table 5.6 Ultimate strength comparison with χ=0.7 and χ=0.94 with available results

Author	ID	P_{EXP} (kN)	CSA			
			P_{CSA} (χ=0.7) (kN)	P_{CSA}/P_{EXP}	P_{CSA} (χ=0.94) (kN)	P_{CSA}/P_{EXP}
YN(1983)	1A	448.8	488.7	1.09	612.8	1.37
YN(1983)	2B	538.2	626.8	1.16	786.1	1.46
YN(1983)	3B	556.8	600.5	1.08	753.0	1.35
YN(1983)	6E	422.6	655.6	1.55	822.1	1.95
			Avg.	1.22		1.53
			COV (%)	18.2		16.4
RD(1984)	2a	210.0	119.4	0.57	154.2	0.73
RD(1984)	2b	410.0	188.4	0.46	270.2	0.66
			Avg.	0.52		0.70
MC(1984)	WA1	471.0	594.7	1.26	740.4	1.57
MC(1984)	WA2	440.0	597.1	1.36	743.4	1.69
MC(1984)	WA3	463.0	575.0	1.24	715.9	1.55
MC(1984)	WA4	476.0	535.3	1.12	666.5	1.40
MC(1984)	WA5	445.0	558.1	1.25	694.8	1.56
			Avg.	1.25		1.55
			COV (%)	6.2		11.4
AM(1985)	WC1	420.0	606.5	1.44	749.0	1.78
AM(1985)	WC2	310.0	614.8	1.98	759.2	2.45
AM(1985)	WC3	285.0	595.8	2.09	735.8	2.58
AM(1985)	WC4	335.0	654.4	1.95	808.2	2.41
AM(1985)	WC5	245.0	617.8	2.52	763.0	3.11
AM(1985)	WC6	365.0	595.8	1.63	735.8	2.02
AM(1985)	WC7	534.0	682.1	1.28	842.3	1.58
AM(1985)	WC8	445.0	673.2	1.51	831.5	1.87
			Avg.	1.80		2.23
			COV (%)	23.4		23.7

Table 5.6 (continued) Ultimate strength comparison with χ=0.7 and χ=0.94 with available results

Author	ID	P_{EXP} (kN)	CSA			
			P_{CSA} (χ=0.7) (kN)	P_{CSA}/ P_{EXP}	P_{CSA} (χ=0.94) (kN)	P_{CSA}/ P_{EXP}
RC(1986)	WD5	334.0	592.5	1.77	717.0	2.15
RC(1986)	WD6	623.0	530.2	0.85	641.6	1.03
RC(1986)	WD7	494.0	513.3	1.04	621.2	1.26
RC(1986)	WD8	200.0	570.4	2.85	690.2	3.45
RC(1986)	WD9	267.0	503.3	1.89	609.0	2.28
RC(1986)	WD10	278.0	518.8	1.87	627.7	2.26
RC(1986)	WD12	196.0	508.7	2.60	615.6	3.14
			Avg.	1.84		2.22
			COV (%)	39.6		39.2
FL(1994)	1	164.0	53.1	0.32	70.6	0.43
FL(1994)	2	173.0	58.3	0.37	77.5	0.45
FL(1994)	3	153.0	69.2	0.45	92.2	0.60
FL(1994)	4	213.0	63.8	0.30	58.5	0.27
FL(1994)	5	172.0	46.1	0.27	61.6	0.36
FL(1994)	9	179.0	93.3	0.52	124.2	0.69
FL(1994)	17	193.0	84.2	0.44	111.1	0.58
FL(1994)	21a	181.0	73.0	0.41	94.5	0.52
			Avg.	0.41		0.49
			COV	25.4		28.1
MH(1996)	SP3	277.7	253.2	0.91	334.6	1.21
MH(1996)	SP4	251.5	88.6	0.35	106.0	0.42
MH(1996)	SP8	190.0	82.2	0.43	102.3	0.54
MH(1996)	SP9	292.8	226.4	0.77	297.2	1.31
MH(1996)	SP10	293.5	112.7	0.38	137.1	0.47
			Avg.	0.56		0.87
			COV	43.7		52.7

Table 5.6 (continued) Ultimate strength comparison with χ=0.7 and χ=0.94 with available results

Author	ID	P_{EXP} (kN)	CSA			
			P_{CSA} (χ=0.7) (kN)	P_{CSA}/ P_{EXP}	P_{CSA} (χ=0.94) (kN)	P_{CSA}/ P_{EXP}
SN(2011)	P1NA	111.0	72.4	0.65	76.7	0.69
SN(2011)	F1NA	156.9	79.4	0.51	99.2	0.63
SN(2011)	P3NA	93.8	53.6	0.57	85.2	0.91
SN(2011)	F3NA	131.7	93.3	0.71	111.3	0.81
SN(2011)	P6NA	104.2	87.9	0.84	125.6	1.21
SN(2011)	P3NI	78.9	66.7	0.85	111.3	1.41
SN(2011)	F3NI	121.9	74.2	0.61	125.6	1.03
			Avg.	0.68		0.96
			COV (%)	19.3		29.5
			Overall Avg.	1.03		1.32
			COV (%)	50.5		50.8

It suggests that using a higher χ factor should be considered in combination with the diagonal strut approach for the infill strength consideration. Although a factor of 0.7 shows some promises, the COV is relatively high. While a 50% of variation is not that unusual in masonry testing, it is recommended that more data points are needed to have more confidence in the value.

CHAPTER 6 SUMMARY AND CONCLUSIONS

6.1 SUMMARY

The behavior and strength of masonry prisms loaded normal and parallel to the bed joint was investigated in this study. The objective of this research is to extend the limited experimental database on the effect of loading direction on compressive strength and to evaluate the design methods in current Canadian and American design standards.

The experimental program included the testing of forty-seven prisms and fifteen panels under compressive loading in the direction normal and parallel to the bed joint. The splitting tensile strength of masonry is also examined by subjecting twelve masonry panels to diagonal compressive loading. One-third scaled standard concrete masonry blocks were used in the construction of the prisms and panels. Parameters included grouting arrangement, mortar strength, height-to-thickness ratio and web interruption. Specimens were tested to failure and the load and displacement data were recorded. The behavior, ultimate load and failure mode were presented and discussed.

The experimental results concerning compressive strength of masonry normal to the bed joint were discussed to illustrate the effects of several parameters such as loading direction, mortar strength, height-to-thickness ratio, grouting and web interruption. The results were then modified according to height-to-thickness correction factors provided by the CSA S304.1-04 (2004) and ASTM C1314 (2011). The experimentally obtained and modified results were used to assess the validity of the "Unit-Mortar Strength" method provided by CSA S304 and MSJC 2011.The horizontal-vertical strength ratio obtained experimentally for panels was used to verify the validity of χ factor provided by CSA S304.1 for the design of infill walls.

6.2 CONCLUSIONS

The following conclusions obtained from this research are presented as follows:

1. Vertically loaded prisms exhibited face-shell spalling and vertical crack through the web and face-shell. Horizontally loaded prisms exhibited some diagonal cracking through face-shell indicating the confining effect. Horizontally loaded panels exhibited cracking through head joints and bed joints of the face-shell.
2. Prisms loaded parallel to the bed joint were found to exhibit higher strength than prisms loaded normal to the bed joint for all grouting configurations and mortar strengths considered. The average horizontal-to-vertical ratio was found to be 1.5.
3. Panels loaded normal to the bed joint were found to exhibit slightly higher strength than panels loaded parallel to the bed joint. The average horizontal-to-vertical strength for panel specimens was found to be 0.94.
4. Grouting decreases prism compressive strength due to the net area calculation, for all loading orientations and mortar strengths. However, grouted specimens have higher load capacity than partially-grouted and hollow specimens.
5. Increasing mortar strength increases prism compressive strength, for all loading orientations and grouting arrangements.
6. The central web is found to contribute to the overall compressive strength of the prism more than the continuous grouted core.
7. Prism height does not seem to have a pronounced effect on the compressive strength of prisms; however this could be due to the small size of the scaled block.
8. Diagonally loaded panels exhibited a stepping crack failure pattern through the mortar joints running through the loaded corner. The diagonal tensile strength increased as the panel grouting percentage increased.
9. Compressive strength obtained from the "Unit-Mortar Strength" method over-estimate the compressive strength when compared with the experimentally obtained prism strength.
10. MSJC 2011 underestimates the strength of infill for all test results considered. In the case of CSA S304.1, it over-estimates the infill strength for very strong infills, but provides conservative values for intermediate and weak infills.

11. The design strength calculated using a χ factor of 0.7 compares better with the test results than using a factor of 0.5. This suggests that a higher χ factor than 0.5 should be considered.

6.3 Recommendations for Further Research

More experiments and research on specimens incorporating a running bond construction such as panel specimens used in this study is required for conducting strength comparison for loading direction. Testing should be done on prisms constructed with stronger mortar strength and results should be compared with the Unit-Mortar Strength Method. Parameters that were not listed in the scope of this study, such as block geometry and variation in block materials should be further studied.

REFERENCES

ACI 530-11/ASCE 5-11/TMS 402-11, (2011). Building Code Requirements for Masonry Structures. USA: Masonry Standards Joint Committee.

Amos, R. (1994). The shear strength of masonry infilled steel frames. M.S. thesis, University of New Brunswick.

ASTM C1314-11a (2011). "Standard Test Methods for Compressive Strength of Masonry Prisms," ASTM International, West Conshohocken, PA.

ASTM C1072-11 (2011). "Standard Test Methods for Measurements of Masonry Flexural Bond Strength," ASTM International, West Conshohocken, PA.

ASTM C140-12 (2012). "Standard Test Methods for Sampling and Testing Concrete Masonry Units and Related Units," ASTM International, West Conshohocken, PA.

ASTM E519 (2010). Standard Test Method for Diagonal Tension (Shear) in Masonry Assemblages, ASTM International, West Conshohocken, PA.

Bennett, R.M., Boyd, K.A. and Flanagan, R.D. (1997). Compressive properties of structural clay tile prisms. Journal of Structural Engineering, 123 (7):920-926.

Boult, B.F. (1979). Concrete masonry prism testing. American Concrete Institute Journal, Proceedings, **76** (4): 513-536.

Brown, R.H. and Whitlock, A.R. (1982). Compressive strength of grouted hollow brick prisms. Masonry: Research, Application, and Problems, ASTM STP 778, pp. 99-117

CAN/CSA A165-04 (2009) - CSA Standards on Concrete Masonry Units. Mississauga, ON, Canada: Canadian Standard Association.

CAN/CSA A179-04 (2009) - Mortar and Grout for Unit Masonry. Mississauga, ON, Canada: Canadian Standard Association.

CAN/CSA S304.1-04 (2004) Design of masonry structures. Mississauga, ON, Canada: Canadian Standard Association.

Drysdale, R.G. and Hamid, A.A. (1979). Behavior of concrete block masonry under axial compression. American Concrete Institute Journal, Proceedings, **76** (6): 707-722.

Drysdale R.G., Hamid, A.A. and Heidebrecht, A.C. (1979). Tensile strength of concrete masonry. Journal of the Structural Division, **105** (7): 1261-1276.

Drysdale, R.G. and Hamid, A.A. (1980). Concrete masonry under combined shear and compression along the mortar joints. American Concrete Institute Journal, Proceedings, **77** (5): 314-320.

Drysdale, R.G. and Hamid, A.A. (1982). Tensile strength of brick masonry. International Journal of Masonry Construction, **2** (4): 172-177.

Drysdale, R.G., and Hamid, A.A. (2005). Masonry structures: Behavior and design. Mississauga, Ontario: Canadian Masonry Design Centre.

Flanagan, R.D. (1994). Behavior of structural clay tile infilled frames. PhD thesis, University of Tennessee, United States.

Flanagan, R. D., and Bennett, R. M. (2001). In-plane analysis of masonry infill materials. Practice Periodical on Structural Design and Construction, **6** (4):176-182.

Guo, P. (1991). Investigation and modeling of the mechanical properties of masonry. PhD thesis, McMaster University.

Haach, V.G., Vasconcelos, G. and Lourenco, P.B. (2010). Influence of the geometry of units and of the filling of vertical joints in the compressive and tensile strength of masonry. Materials Science Forum, **636**:1321-1328.

Hamid, A.A., Abboud, B.E. and Harris, H.G. (1985). Direct modeling of concrete block masonry under axial compression. Masonry: Research, Application, and Problems, ASTM STP 871, pp. 151-166.

Hamid, A.A. and Abboud, B.E. (1986). Direct modeling of concrete block masonry under shear and in-plane tension. ASTM International, **14** (2):112-121.

Hatzinikolas, M. and Korany, Y. (2005). Masonry design for engineers and architects. Edmonton, Alberta: Canadian Masonry Publications.

Hegemier, G.A., Krishnamoorthy, G., Nunn, R.O. and Moorthy, T.V. (1978). Prism tests for the compressive strength of concrete masonry. Proceedings of the North American Masonry Conference, paper 18, pp. 18-1 – 18-17.

Hedstorm, E.G. and Hogan, M.B. (1990). The properties of masonry grout in concrete masonry. Masonry: Components to Assemblages, ASTM STP 1063, pp. 47-62.

Johnson, F.B. and Thompson N. (1969). Development of diametral testing procedures to provide a measure of strength characteristics of masonry assemblages.

Khalaf, F.M. (1997). Blockwork masonry compressed in two orthogonal directions. Journal of Structural Engineering, **123** (5):591-596.

Korany, Y. and Glanville, J. (2005). Comparing masonry compressive strength in various codes. Concrete International, **27** (7):35-39.

Lee, R., Longworth, J. and Warwaruk J. (1984). Concrete masonry prism response due to loads parallel and perpendicular to bed joint. Department of Civil Engineering, University of Alberta.

Maleki, M., Hamid, A.A., El-Damatty, A.A. and Drysdale, R.G. (2007). Behavior of partially grouted reinforced concrete masonry panels under in-plane diagonal loading. Proceedings of the 10th North American Masonry Conference. pp. 1039-1050.

McBride, R. (1984). The behavior of masonry infilled steel frames subjected to racking. M.S. thesis, University of New Brunswick.

Mehrabi, A.B., Shing, P.B., Shuller, M.P. and Noland J.L. (1996). Experimental evaluation of masonry-infilled RC frames. Journal of Structural Engineering, **122** (3): 228-237.

Menash, P. and Liu, Y. (2013). Concrete masonry steel infilled frames subjected to combined in-plane lateral and axial loading- an experimental study. Journal of Engineering Structures, **55** (7): 331-339.

Mosalam, K.M.A. (1996). Experimental and computational strategies for the seismic behavior evaluation of frames with infill walls. PhD thesis, Cornell University, United States.

Mota, M.C., Minaie, E., Golecki, T., Holly, E., Moon, F.L. and Hamid, A.A. (2007). Diagonal tension strength of partially grouted concrete masonry assemblages. Proceedings of the 10th North American Masonry Conference. pp. 1027-1038.

Richardson, J. (1986). The behavior of masonry infilled steel frames. M.S. thesis, University of New Brunswick.

Riddington, J. R. (1984). The influence of initial gaps on infilled frame behavior. Proceedings of the Institution of Civil Engineers, **77** (3):295-310.

Soon, S. (2011). In-plane behavior and capacity of concrete masonry infills bounded by steel frames. M.S. thesis, Dalhousie University.

Steadman, M., Drysdale, R.G. and Khattab M.M. (1995). Influence of block geometry and grout type on compressive strength of block masonry. Seventh Canadian Masonry Symposium, pp. 1116-1127.

Wong, H.E. and Drysdale, R.G. (1985) Compression Characteristics of Concrete Block Masonry Prisms. Masonry: Research, Application, and Problems, ASTM STP 871, pp. 167-177.

Yong, T.C. (1983). Shear strength of masonry infilled panels in steel frames. M.S. thesis, University of New Brunswick.

APPENDIX A – SAMPLE CALCULATIONS

The following section presents a step-by-step design strength calculation according to both the CSA S304.1-04 and MSJC 2011 standards. The specimen under consideration is "1a" by YN (1983). The properties of the frame and infill are shown in the table below.

Table A. 1 Frame and infill properties of specimen 1A (Yong 1983)

Specimen: 1A			
Frame Properties		Infill Properties	
E_b =	200,000 MPa	f'_m =	23.7MPa
E_c =	200,000 MPa	E_m =	20,000 MPa
I_b =	$4.54 \times 10^7 mm^4$	h_w =	2,800 mm
I_c =	$1.88 \times 10^7 mm^4$	l_w=	3,600 mm
		t =	190 mm
		t_f =	33 mm

A. 1 STRENGTH CALCULATIONS ACCORDING TO CSA S04.1-04

The width of the equivalent diagonal strut:

$$\alpha_h = \frac{\pi}{2}\sqrt[4]{\frac{4E_f I_c h_w}{E_m t_e \sin 2\theta}}$$ Equation [2.3]; $$\alpha_l = \pi\sqrt[4]{\frac{4E_f I_b l_w}{E_m t_e \sin 2\theta}}$$ Equation [2.4]

$$\alpha_h = \frac{\pi}{2}\sqrt[4]{\frac{4(200{,}000)\ \ (1.88\text{x}10^6)\,(2{,}800)}{(20{,}000)\,(66)\sin 2(0.661)}} = 669.0 \text{ mm}$$

$$\alpha_L = \pi\sqrt[4]{\frac{4(200{,}000)\ \ (4.54\text{x}10^6)(3{,}600)}{(20{,}000)\,(66)\sin 2(0.661)}} = 1{,}776.3 \text{ mm}$$

Where,

$t_e = 2t_f = 66$ mm,

$$\theta = \tan^{-1}\left(\frac{h_w}{l_w}\right) = \tan^{-1}\left(\frac{2{,}800}{3{,}600}\right) = 0.661$$

$$w_e = \frac{w}{2} = \frac{1}{2}\sqrt{\alpha_h^2 + \alpha_L^2} \quad \text{Equation [2.7]}$$

$$w_e = \frac{1}{2}\sqrt{(669.)^2 + (1{,}776.3)^2} = 949.1 \text{ mm}$$

$$l = \sqrt{(2{,}800)^2 + (3{,}600)^2} = 4{,}560.7 \text{ mm}$$

Ratio $\frac{w/2}{l} = \frac{949.1}{4{,}560.7} = 0.208 < 0.25$

CSA S304.1-04 cl. 7.13.3.3 states that the effective width shall not exceed 0.25 of the diagonal length; hence the effective strut width is 948.3 mm.

The length of the strut for slenderness effect is calculated as follows according to CSA S304.01-04 cl.7.13.3.4:

$l_d = 4{,}560.7 - 0.25(949.1) = 3{,}611.6$ mm

The slenderness of the strut is calculated as follows:

$$\frac{kl_d}{t} = \frac{0.9x3{,}611.6}{190} = 17.1 < 30, \text{ ok}$$

Where,

k =0.9 (CSA S304.1 Annex B)

The diagonal load in the strut, Pr-hollow, is calculated as follows, according to equation [2.6]:

$$P_{r-Hollow} = \phi_m \chi (0.85 f'_m) b(2t_f - r)$$

Where,

$\phi_m = 1$

$\chi = 0.5$ (CSA S304.1 cl 10.2.6),

b = w/2 = 949.1 mm,

$t_f = 33$ mm

As shown in Equation 7.30 in section 7.4.4 from Drysdale and Hamid (2005), the value for r is calculated as follows:

$$r = \left(\frac{t}{2} + e\right) - \frac{1}{2}\sqrt{t^2 + 4te + 4e^2 - 16et_f} = \left(\frac{190}{2} + 19\right) - \frac{1}{2}\sqrt{190^2 + 4(190)(19) + 4(19^2) - 16(19)(33)}$$

r =11.6

Where,

e is taken as minimum eccentricity = 0.1t = 0.1(190) = 19 mm

Hence,

$$P_{r-Hollow} = \phi_m \chi (0.85 f'_m) b(2t_f - r) = 1.0(0.5)(0.85x23.7)(949.1)\left[(2x33) - 11.6\right] = 520.1 \text{ kN}$$

Considering slenderness, CSA S304.1 cl.7.7.6.3 provides the following equation for calculating

The critical axial compressive load, P_{cr}:

$$P_{cr} = \frac{\pi^2 \phi_e (EI)_{eff}}{(kh)^2 (1 + 0.5\beta_d)}$$

where,

$\phi_e = 0.65$ for unreinforced masonry,

$\beta_d = 0$ for temporary loading,

$(EI)_{eff} = 0.4E_mI_o = 3.13\text{x}10^{12}$ Nmm^2

$$I_o = \frac{(b)(t^3 - (t - 2t_f)^3)}{12} = 3.91\text{x}10^8 \text{ mm}^2$$

$$P_{cr} = \frac{\pi^2 0.65(3.13x10^{12})}{(0.9x3{,}611.6)^2[1+0.5(0)]} = 1902.5 \text{ kN}$$

CSA S304.1-04 cl.7.7.6.3 outlines the moment magnifier method for the magnification eccentricity e′. An iteration process is required between e and e′ until they converge. The first iteration of e′ is as follows.

$$e' = \frac{1}{1-\left(\frac{P_r}{P_{cr}}\right)} e = \frac{1}{1-\left(\frac{520.1}{1902.5}\right)} e = 1.375e \text{ ; Ratio } e'/e = 1.375$$

The ratio for the first iteration of e′ is obtained and is then multiplied to e. e is then replaced by the new e′ in the r equation to reiterate the results as follows:

$$r = \left(\frac{190}{2} + 19x1.375\right) - \frac{1}{2}\sqrt{190^2 + 4(190)(19x1.375) + 4((19x1.375)^2) - 16(19x1.375)(33)}$$

r =15.2

After several iterations, the final P_r is calculated to be 487.4 kN. The horizontal force that can be resisted in the horizontal component, V_r, is then calculated as follows:

$$V_r = \frac{1}{\sqrt{h_w^2 / l_w^2}} P_r = \frac{1}{\sqrt{2{,}800^2 / 3{,}600^2}} 487.4 = 384.7 \text{ kN}$$

Using S-Frame, a linear static analysis was performed in order to obtain the horizontal coefficient. When a 1kN force was applied at the roof level of the beam, the horizontal component of the force in the diagonal strut obtained from the analysis was 0.97 kN. Therefore, to obtain the actual capacity of the frame, the ultimate strength is divided by the horizontal coefficient as follows.

$$V_{ult-\text{mod}} = \frac{V_{r-ult}}{0.97} = \frac{384.7kN}{0.97} = 396.6 \text{ kN}$$

A. 2 STRENGTH CALCULATIONS ACCORDING TO MSJC 2011

The width of the equivalent diagonal strut:

$$\lambda_{strut} = \sqrt[4]{\frac{E_I t_e \sin 2\theta}{4E_c I_c h}} = \sqrt[4]{\frac{(20{,}000)(66)\sin 2(0.661)}{4(20{,}0000)(1.88x10^6)(2{,}800)}} = 0.002349 \text{ Equation [2.8]}$$

$$w_{\inf} = \frac{0.3}{\lambda_{strut}\cos\theta} = \frac{0.3}{0.002349x\cos(0.661)} = 161.8 \text{ mm Equation [2.7]}$$

The vertical load, P_{ult}, is calculated as follows, according to equation [2.9]:

$$P_{ult} = (152.4\text{ mm})t_{netinf}f'_m = 152.4(66)(23.7) = 238.0kN = 238.0 \text{ kN}$$

Using S-Frame, a linear static analysis was performed as discussed earlier and the horizontal coefficient was found to be 0.82. The actual capacity of the frame is as follows:

$$P_{ult-\text{mod}} = \frac{P_{ult}}{0.97} = \frac{238.0kN}{0.82} = 290.2 \text{ kN}$$